REPUBLIC OF TURKEY
YILDIZ TECHNICAL UNIVERSITY
GRADUATE SCHOOL OF NATURAL AND APPLIED SCIENCES

DETECTION AND CLASSIFICATION OF NUCLEI IN HISTOPATHOLOGICAL IMAGES

Roaa Safi ABED ALAH

MASTER OF SCIENCE THESIS
Department of Computer Engineering
Program of Computer Engineering

Advisor
Assoc. Prof. Dr. Gokhan BILGIN

July, 2019

REPUBLIC OF TURKEY
YILDIZ TECHNICAL UNIVERSITY
GRADUATE SCHOOL OF NATURAL AND APPLIED SCIENCES

DETECTION AND CLASSIFICATION OF NUCLEI IN HISTOPATHOLOGICAL IMAGES

A thesis submitted by Roaa Safi ABED ALAH in partial fulfillment of the requirements for the degree of **MASTER OF SCIENCE** is approved by the committee on 22.07.2019 in Department of Computer Engineering, Program of Computer Engineering .

Assoc. Prof. Dr. Gokhan BILGIN
Yildiz Technical University
Advisor

Approved By the Examining Committee

Assoc. Prof. Dr. Gokhan BILGIN, Advisor
Yildiz Technical University _____

Asst. Prof. Dr. Zeyneb KURT , Member
Yildiz Technical University _____

Asst. Prof. Dr. Sefer BADAY , Member
İstanbul Technical University _____

I hereby declare that I have obtained the required legal permissions during data collection and exploitation procedures, that I have made the in-text citations and cited the references properly, that I haven't falsified and/or fabricated research data and results of the study and that I have abided by the principles of the scientific research and ethics during my Thesis Study under the title of DETECTION AND CLASSIFICATION OF NUCLEI IN HISTOPATHOLOGICAL IMAGES supervised by my supervisor, Assoc. Prof. Dr. Gokhan BILGIN. In the case of a discovery of false statement, I am to acknowledge any legal consequence.

Roaa Safi ABED ALAH

Signature

ACKNOWLEDGEMENTS

Foremost, I would like to express my sincere gratitude to my advisor Assoc. Prof. Dr. Gokhan BILGIN for the continuous support for me, for his patience, motivation, enthusiasm and his knowledge. His guidance helped me a lot to complete and finalizing this research.

Besides my advisor, I would like to thank the rest of my thesis committee: Asst. Prof. Dr. Sefer BADAY and Asst. Prof. Dr. Zeyneb KURT.

My thanks also goes to Dr. Abdulkadir Albayrak, and all staff in our department at Yıldız Technical University.

Last but not least, I would like to thank my parents especially, my precious mother Hutham Al-Asadi for her supporting and patience in all my life, also, my thank to my wonderful sisters.

Roaa Safi ABED ALAH

TABLE OF CONTENTS

LIST OF SYMBOLS vii

LIST OF ABBREVIATIONS viii

LIST OF FIGURES x

LIST OF TABLES xiii

ABSTRACT xiv

ÖZET xvi

1 Introduction 1

1.1 Literature Review 2

1.2 Objective of The Thesis 5

1.3 Hypothesis 6

2 General Information 7

2.1 Machine Learning (ML) 7

2.1.1 Types of machine learning 8

2.1.2 Conventional artificial neural network (ANN) 9

2.1.3 Deep learning 12

2.1.4 Convolutional neural networks (CNNs) general description . . 13

2.2 Computer Vision 16

2.2.1 Object detection and classification 17

3 Detection of Nuclei in Histopathological Images 18

3.1 Detection of Nuclei 18

3.2 Experimental Data Set 19

3.3 Fuzzy C-means Clustering Algorithm 21

3.4 Nuclei Detection in Histopathological Images via Fuzzy C Means Clustering Method and Convolutional Neural Network. 23

3.4.1 Nuclei center detection via fuzzy c-means clustering algorithm. 24

3.4.2 Experimental results obtained by fuzzy c means clustering method 30

3.4.3 Nuclei center detection via tiny convolutional neural networks (Tiny-CNN) . . . 32
3.4.4 Detection and evaluation results obtained by tiny-CNN 37
3.4.5 Nuclei center detection via combined (FCM) unsupervised method with (CNNs) supervised method. . . . 38
3.4.6 Evaluated results of nuclei center detection via combined (FCM) unsupervised method with supervised method 39
3.5 Discussions . . . 42

4 Classification of Nuclei in Histopathological Images **44**
4.1 Data Set and Prepossessing in Histopathological Images . . . 44
4.2 Local Phase Quantization (LPQ) . . . 47
4.3 Nuclei Classification in Histopathological Images via Local Phase Quantization and Convolutional neural network . . . 48
4.3.1 Nuclei classification in histopathological images via local phase quantization and support vector machine . . . 48
4.3.2 Nuclei classification via convolutional neural network and support vector machine . . . 50
4.3.3 Evaluated the performance results of nuclei classification . . . 52
4.3.4 Summary of nuclei classification in histopathological images . . 55

5 Result and Discussion **56**
5.1 Result and Discussion . . . 56
5.2 Future Works . . . 57

References **58**

Publications From the Thesis **64**

LIST OF SYMBOLS

$\hat{y}$	Predicting y
b	Bias
$\varphi(.)$	Activation function
j	Number of clusters
$\widehat{(B)}$	Represents a reflection of the structuring element B
$\otimes$	2D convolution operator
x_i	The objects in the cluster
m	Any real number bigger than 1
l	Number of layers
f_l	Defines as activation function
${k_n}^l$	Feature map output
$H^{(l-1)}W^{(l-1)}$	Pixels, size of mask convolution mask
$z_n^{(l-1)}$	A matrix of the result calculated from the four pixels in layers
N^L	Number of output layers
$w_{m,n}^L$	Weight from feature map
K	Multi-dimensional filters
(fH)	Filter height
(fW)	Filter width
(DD')	Number of filters in the bank
S_h	A subampling stride
P_h^-, P_h^+	The amount of zero padding
w_u	Basis vector of the $2-D$
I	Image size(m,n)

LIST OF ABBREVIATIONS

ANN	Artificial Neural Network
CNN	Convolutional Neural Network
CRC	Colon Routine Cancer
CAD	Computer Aided Diagnosis
DL	Deep Learning
DSC	Dice Similarity Coefficient
d_ij	Distance between pixel i and i
FCM	Fuzzy C Means
FP	Fouls Positive
FN	Fouls Negative
F-M	F Measure
ICA	Independent Component Analysis
Im	Imaginary vector
GPU	Graphical Processing Unit
GT	Ground Troth
$H\&E$	Hemotoxylin and Eosin
K-Means	Kernel means
LPQ	Local Phase Quantization
LoG	Laplacian of Gaussian
ML	Machine Learning
MSE	Mean Squire Error
Neg	Negative
PCA	Principal Component Analysis

Pos	Positive
PPR	Positive Prediction Rate
P_H	Padding number of zero height
P_W	Padding number of zero width
ROI	Region of Interest
ReLU	Rectified Linear Unit
RGB	Red Green Blue
Re	Real vector
SGD	Stochastic Gradient Decent
STFT	Short Term Fourier Transform
STD	Standard deviation
SVM	Support Vector Machine
Tiny-CNN	Tiny Convolutional Neural Network
TIA	Tissue Image Analytic
TPR	True Positive Rate
TP	True Positive
UCSB	University of California Santa Barbara's
U	Total number of pixel in image

LIST OF FIGURES

Figure 2.1 Basic scenario of neuron in artificial neural network 10
Figure 2.2 The sigmoid function 11
Figure 2.3 The tanh function 12
Figure 2.4 The output feature map of CNNs 14
Figure 2.5 The convolution layer in CNNs 15
Figure 2.6 The pooling layer in CNNs 15
Figure 3.1 Data set (a) original image, (b) ground truth image (a), (c) original image, (d) ground truth image (d) 20
Figure 3.2 (a) original image (UCSB- data set), (b) (x,y) data set (c) original ground truth image 20
Figure 3.3 (a) original image (CRC- data set), (b) (x,y) data set 21
Figure 3.4 Flowchart proposed methodology 23
Figure 3.5 Regional outputs of five different clusters obtained by FCM algorithm 25
Figure 3.6 (a) Five different cluster regions of FCM algorithm (b) obtained nuclei cluster of FCM approach with maximum standard deviation and(c) final output nuclei centers image. 26
Figure 3.7 Sequence steps of fuzzy c means automatic and semi-automatic approaches for detecting the center of nuclei in histopathological images 27
Figure 3.8 (a) Standard deviation results for each cluster illustrated the intensity value for each cluster (b) select the best cluster manually (semi-automatic) 28
Figure 3.9 a) An original image from UCSB-58 data set, (b) its ground-truth, (c) FCM result after choosing closest cluster manually, d) FCM result after morphological operation, (e) FCM nuclei center detection and (f) masked image of nucleus with center detection . 29
Figure 3.10 Standard deviation results for each cluster illustrated the intensity value for each cluster 30
Figure 3.11 (a) Original image, (b) Center image obtained from FCM-automatic (c) Original image obtained from FCM-semiautomatic. 31

Figure 3.12 (a) Positive blobs, (b) Negative blobs 33
Figure 3.13 Tiny-CNN learning to detect center of nuclei in histopathological image 36
Figure 3.14 (a) Original image UCSB data set, (b) filtered nuclei in tiny-CNN process, (c) center nuclei in tiny-CNN process (d) mask nuclei after tiny-CNN 36
Figure 3.15 (a) Original image UCSB data set, (b) center nuclei after Tiny-CNN process 37
Figure 3.16 (a) Original image from UCSB-58 data set, (b) the result of filtering, (c) Tiny-CNN output image detect of nuclei, (d) final output result of Tiny-CNN detect center of nuclei, (e) FCM semiautomatic result, (f) generated mask from the FCM semiautomatic result combined with original image g) used mask image with Tiny-CNN output the center of the nuclei detection 38
Figure 3.17 (a) Boundary of cell size in UCSB data set to detect the correct nuclei, (b) boundary if cell size in CRC data set to detect the correct nuclei in histopathological images 39
Figure 3.18 a) An example image of UCSB-58 data set and, b) red points represent outputs of nucleus center detection by Tiny-CNN; green circles refer to ground truth information. c) An example image of CRC-100 data set and, d) output of detected nucleus centers Tiny-CNN and ground-truth 41
Figure 3.19 Result of all the methods of the first approach on the UCSB data set 42
Figure 3.20 Result of all the methods of the first approach on the CRC data set 43
Figure 4.1 (a,b,c,d) four different types of nuclei, (e) the original image of histopathological images 45
Figure 4.2 Example of data set patches consist of four types of nuclei stand as: (a) epithelial, (b) fibroblast, (d) inflammatory, (c) others. 46
Figure 4.3 Proposed a histopathological patches images after applying augmented methods. 46
Figure 4.4 selected features by proposed a histogram on three orthogonal levels 47
Figure 4.5 Flowchart proposed LPQ-SVM methodology 49
Figure 4.6 Spatial localization of the selected features by proposed a histogram on three orthogonal levels 50
Figure 4.7 ResNet convolutional neural network based model to classify four types of cells in histopathological images along with augmented data set. 51

Figure 4.8 Confusion matrices: (A) Confusion matrices of CNN models applied to the augmented data set with ResNet101 for CNN based feature extraction to classify epithelial and other classes, (B) Confusion matrices ResNet101 for CNN based feature extraction to classify inflammatory and fibroblast classes, (C) Confusion matrix using ResNet50 for classify inflammatory and fibroblast, (D) Confusion matrices for classify epithelial and other based on augmented data set. 53
Figure 4.9 Confusion matrices for CNN-SVM based model to classify four types of cells in histopathological images along with augmented data set. 53
Figure 4.10 Confusion matrices for LPQ-SVM based model to classify four types of cells in histopathological images along with augmented data set. 54
Figure 4.11 Confusion matrices for LPQ-SVM based model for two classes (a) epithelial and fibroblast (b) inflammatory and others with original data set. 54
Figure 4.12 Flowchart of the proposed framework of the second part 55

LIST OF TABLES

Table 3.1 Fuzzy c means results to detect center of nuclei using two different size of histopathological images 31
Table 3.2 Nuclei Center Detection Results with UCSB-58 and CRC-100 Histopathological Image Data Sets by using Automated Method Tiny-CNN 37
Table 3.3 Nuclei detection results with UCSB-58 and CRC-100 histopathological image data sets by using Tiny-CNN and FCM semiautomatic, automatic method, and, combined FCM semiautomatic with Tiny-CNN 41
Table 3.4 Comparative results for nucleus detection with other studies 42
Table 4.1 Information Table of Augmented Data Set 45
Table 4.2 Results of Confusion Matrix with Original Data Set Using CNN-SVM 52
Table 4.3 Results of Confusion Matrices with Augmented Data Set Using CNN-SVM 52

ABSTRACT

DETECTION AND CLASSIFICATION OF NUCLEI IN HISTOPATHOLOGICAL IMAGES

Roaa Safi ABED ALAH

Department of Computer Engineering
Master of Science Thesis

Advisor: Assoc. Prof. Dr. Gokhan BILGIN

Histopathology is the study of tissues from body under the microscope to analyze and characterize a disease. If we separate the words of histopathology, the study of tissues is called as histology, and the study of disease is called as pathology, Therefore, histopathology refers to the study of tissues associated with diseases. In this study, the automated analysis of cellular structures has been studied in histopathological images; whereas the conventional manual methods are relatively expensive and time-consuming workload for pathologists. Recently, computers have aided the researches on the diagnostic algorithms which have obtained a high significance for pathologists in extracting the cellular structures from histopathological images. In this thesis, we have proposed two approaches for detecting and classification of nuclei in histopathological images. Firstly, we have detected the centers of nuclei in histopathological images, which is a hard problem for computers, based on two methods. The first method is composed of two main stages: starting with fuzzy c-means (FCM) algorithm in pre-segmentation, then detection nuclei centers with tiny-convolutional neural network (Tiny-CNN). At that point, the unsupervised method (FCM) is combined with supervised method (Tiny-CNN) to find more information about the cellular structures in the related tissue. In the second method, the deep learning method is used to detect the center of nucleus directly. Afterwards, each of these individual methods is combined to extract more details about the cell structure in histopathological images. Experiments are conducted on two different data sets: namely University of California Santa Barbara's UCSB-58 data set and data set University of Warwick's CRC-100 data set. For the second approach in

this study, we proposed the nuclei classification in histopathological images. The classification of nuclei patterns in histopathological images has attracted a significant interest in a wide range of biomedical research. In recent years, developments in deep learning approaches have solved different issues and shown promising results on histopathological images. These developments have assisted researchers to distinguish between different types of pathological nuclei samples without high labeling costs. In a manuel routine examinations, analysis of histopathological slides under a microscope might be sensitive, slow and inaccurate due to the subjective evaluations. In the context of this part of the thesis, we have aimed at two different types of machine learning approaches for automatic nuclei classification in histopathological images. We have used the University of Warwick's colon data set in the experiments with four nuclei types: epithelial, inflammatory, fibroblast and other type. In the first approach, a convolutional neural network is used for feature extraction, and classification model has been obtained with support vector machine method. In the second approach, local phase quantization (LPQ) is utilized along with support vector machine-based classification with applying a data set augmentation. As a conclusion we can say that the obtained results are achieved high accuracy rates on the detection and classification of nuclei in histopathological images.

Keywords: Histopathological images, nuclei detection, nuclei classification, fuzzy c-means (FCM) algorithm, convolution neural networks, deep learning, local phase quantization.

ÖZET

HİSTOPATOLOJİK GÖRÜNTÜLERDE TESPİT VE SINIFLANDIRMA NÜKLELERİ

Roaa Safi ABED ALAH

Bilgisayar Mühendisliği Anabilim Dalı
Yüksek Lisans Tezi

Danışman: Doç. Dr. Gökhan BILGIN

Histopatoloji, bir hastalığın analiz ve karakterize edilmesi için vücuttan alınan dokuların mikroskop altında incelenmesidir. Histopatoloji kelimesini sözcüklerine ayırırsak, doku incelemesi histoloji, hastalık çalışması ise patoloji olarak adlandırılır. Bu nedenle, histopatoloji hastalıklarla ilgili dokular üzerinde çalışılması anlamına gelir. Bu çalışmada, hücresel yapıların otomatik analizi histopatolojik görüntülerde incelenmiştir; geleneksel manuel yöntemler ise patologlar için nispeten pahalı ve zaman alan bir iş yüküdür. Son zamanlarda bilgisayarlar, hücresel yapıların histopatolojik görüntülerden çıkarılmasında patologlar için yüksek öneme sahip olan tanısal algoritmalar üzerine yapılan araştırmalara yardımcı olmuştur. Bu tezde, histopatolojik görüntülerde çekirdeklerin tespiti ve sınıflandırılması için iki yaklaşım önerilmiştir. İlk olarak, iki yöntemle bilgisayarlarda zor bir problem olan histopatolojik görüntülerde çekirdek merkezlerini tespit edilmiştir. İlk yöntem iki ana aşamadan oluşur: bulanık c-ortalama (BCO) algoritmasıyla ön bölütleme ve sonrasında küçük evrişimsel sinir ağı (Tiny-CNN) ile çekirdek merkezlerinin tespiti. Bu noktada, eğiticisiz yöntem (FCM), ilgili dokudaki hücresel yapılar hakkında daha fazla bilgi bulmak için eğiticili yöntem (Tiny-CNN) ile birleştirilmiştir. İkinci yöntemde, derin öğrenme yöntemi çekirdeğin merkezini doğrudan tespit etmek için kullanılmıştır. Daha sonra, bu yöntemlerin her biri, histopatolojik görüntülerde hücre yapısı hakkında daha fazla ayrıntı çıkarmak için birleştirilir. Deneyler iki farklı veri kümesi üzerinde gerçekleştirilmiştir: Kaliforniya Üniversitesi Santa Barbara'nın UCSB-58 veri kümesi ve University of Warwick'in CRC-100 veri kümesi. Bu çalışmada ikinci yaklaşım olarak, histopatolojik görüntülerde çekirdek sınıflamasını önerilmiştir. Çekirdek

örüntülerinin histopatolojik görüntülerde sınıflandırılması, geniş bir yelpazedeki biyomedikal araştırmalarda büyük ilgi çekmektedir. Son yıllarda, derin öğrenme yaklaşımlarındaki gelişmeler farklı sorunları çözmüş ve histopatolojik görüntüler üzerinde ümit verici sonuçlar göstermiştir. Bu gelişmeler araştırmacılara, yüksek etiketleme maliyetleri olmadan farklı patolojik çekirdek örnekleri arasındaki farkı ayırt etmelerinde yardımcı olmuştur. Manuel bir rutin incelemede, mikroskop altında histopatolojik slaytların analizi, subjektif değerlendirmeler nedeniyle hassas, yavaş ve yanlış olabilir. Tezin bu bölümünde, histopatolojik görüntülerde otomatik çekirdek sınıflaması için iki farklı tipte makine öğrenme yaklaşımı hedeflenmiştir. Yapılan deneylerde Warwick Üniversitesi'nin dört farklı çekirdek tipine sahip kolon verilerini kullandık: bu sınıflar epitelyal, enflamatuar, fibroblast ve diğer türleridir. İlk yaklaşımda, özellik çıkarımı için evrişimli bir sinir ağı kullanılmış ve destek vektör makinesi yöntemiyle sınıflandırma modeli elde edilmiştir. İkinci yaklaşımda, lokal faz nicelemesi (LFN), bir veri kümesi büyütme uygulayarak destek vektör makine temelli sınıflandırma ile birlikte kullanılmıştır. Sonuç olarak, elde edilen sonuçların histopatolojik görüntülerde çekirdeklerin tespiti ve sınıflandırılmasında yüksek doğruluk oranlarına ulaştığını söyleyebiliriz.

Anahtar Kelimeler: Histopatolojik görüntüler, çekirdek tespiti, çekirdek sınıflandırma, bulanık c-ortalamalar (BCO) algoritması, evrişimsel sinir ağları, derin öğrenme, yerel faz nicelemesi.

1
Introduction

At the present time, an increasing number of software technologies that are specialized in artificial intelligence, machine learning, and deep learning has led development to increase interest in these topics. In addition, experts working in this area cannot reach consensus on these words and new concepts occur in this field. Along with the proceeding technology, artificial intelligence that enters the center of our lives, the machine learning that regulates the decision-making mechanism of the computers and the data analysis and algorithms under all these deep learning are progressing not only in engineering but also in many disciplines as a common future field of study. These studies, which are called artificial intelligence, have a direct effect on life and technology. With programming languages, we are able to program devices with a large range of processors. These devices basically implement the commands that are received from us at the same time through their systems. This is the most important part of the technology to go so far with the perfect functioning programmable feature. For example, it is easy to understand and solve the structures consisting of repetitions, control groups or mathematical operations; the current technology remains inadequate the one which requires logic to be executed. In this way, Deep Learning is the basis for teaching and learning methods in this system. Based on the artificial intelligence learning, the process of analyzing and analyzing the image which is called the big data is after the process from the algorithm and data sets to the machine learning. To process this big information of data, it is important to reach more information about the content of images, a piece of information based on automated methods which is useful for a wide variety of images. In this work, we will experiment with a medical image, especially histopathological images. Histopathological image analysis has various challenges, especially in nucleus detection and classification. The developments in techniques that have been occurred in this area can be a valuable assistance to the accurate pathological diagnosis. However, it is still harder to reach more details without solving the main complicated issues in cellular structures especially the clustering problem in tissue. The cellular structure analysis is significant in pathological diagnoses of breast cancer which depends on cell analysis separately. In

medical image technology, it becomes possible to reach more information by modifying the pre-processing of histopathological images. Additionally, the development in this area assists with processing data without the need of data labeling. Machine learning enables classification and clustering by using supervised and unattended methods.

1.1 Literature Review

Computer based image and vision methods lead the development of assisted screening systems to find the information of images and videos as similar to human vision system [1]. The developments in computer-aided methods have revealed new challenges for machine learning performances such as learning from structured descriptions. Moreover, histopathological image analysis has various challenges, especially in nucleus detection and classification. The developments in techniques that have been occurred in this area can be a valuable assistance to the accurate pathological diagnosis. However, it is still harder to reach more details without solving the main complicated issues in cellular structures especially the cluttering problem in tissue [2], in many cases the cells are surrounded by clutter represented by complex histological structures, for example: capillaries, adipocytes, collagen and etc. The cellular structure analysis is significant in pathological diagnoses of breast cancer which depends on cell analysis separately [3]. The examination of the naturally occurring cell types and the condition of the tissue architecture use several complex steps in histopathological images, they use conventional manual methods, and also, a relatively expensive and time consuming work for pathologists. Recently, computer has aided and facilitated research for the diagnostic algorithms which have obtained a high significance to assist the pathologists to extract cellular structures. Cell structure is important for quantitative diagnosis of tissues; moreover, it is needed for regularities of cell shapes in tissue. In this section of the study, we provided the recent techniques for the detection and classification nuclei in pathological images. Traditionally, nuclei identification is a classical issue of histopathological images. Recent studies have implemented conventional methods, various ways of deep learning scenarios, and scenarios connecting both methods. A graph-cut method took place by multi-scale filtering Laplacian of Gaussian (LoG), adaptive scale selection, and a second graph-cut operation [4]. Nucleus detection in recent year, using pre-processing morphological methods assists to smooth and remove non-nuclei objects from input images. Generalized LoG filters and mean-shift clustering were employed to detect nuclei seeds centers and false nucleus were removed by adaptive thresholding [5]. Generalized LoG (gLoG) filters were applied to develop correctly estimated nucleus shape detector performance and it used watershed segmentation technique to separate nucleus and count cells [6]. The domain of FCM for detecting

nucleus positions of feature similarity index measure FSIM is used as seeds for segmentation, this method is started with FCM clustering and then using FSIM based on the template matching approach for nucleus detection. FCM in probabilistic model and a derivation of an algorithm for FCM clustering is supplied expanded ability through the conventional FCM [7]. This study which is known as Bayesian Fuzzy Clustering that has extended each of variable group of clusters and a particle filters dedicated techniques to evaluate the model parameter included the number of clusters [8]. In recent years, the development in machine learning methods is displayed an effective way of detecting a cell in an image by predicting for each pixel position. One of these methods has discovered the location of each pixel that is the monotonous function of the distance to evaluate the closest nuclei to the center. Then the nuclei center can be specified by extracting local extremism of the predicted values [9]. While Stacked Sparse Autoencoder (SSAE) method is presented to solve the complexity of automated nuclei detection, a deep learning method is applied to detect effective nuclei on high-resolution histopathological images of breast cancer which is learning high-level features in just one-pixel intensity to recognize distinctive features of nucleus with good results [10]. A model is proposed the convolution neural networks for detecting the nuclei cells in images with overlapped cells. CNN is trained from all patches extracted from the training images, which the center of pixel in training patch is classified to three classes: background, cytoplasm, and nucleus. To make a network, one should learn how to guess right classification of each central pixel of the patches [11]. This method applied the colour deconvolution to reconstruct all of the applied stains. In addition, the structure of a highest feature set and modification is applied the AdaBoost method to create two detectors that focused on various features in the nuclei and modified of AdaBoost, it enables to calculate the cost of each feature during the selection of nuclei. The output of each detector is incorporated by the optimal active contour algorithm to smooth the border of detected nuclei [12].

A convolution neural network with the LoG filter is applied to histopathological images for performing nuclei detection by sliding window to whole image. Application of this algorithm in histopathogical images performs promising results in nucleus detection [13]. The CNN-based deep learning algorithm with superpixel analysis has shown improved segmentation performance for nuclei segmentation while comparing with the state-of-the art methods. This method over-segments the original image by generating superpixels which allow the CNN to learn the localized features better in the training stage. In another study, Spatially Constrained Convolutional Neural Network (SC-CNN) which forced spatial constraint at the prediction of the likelihood of a pixel by locating higher probability values to the pixels located in the vicinity of the nuclei centers this was implemented for nucleus detection. In that study the

classification of nuclei is presented a Neighboring Ensemble Predictor method (NEP) combined with convolution neural network. That provides a good availability in the results of joint classification, detection of the proposed SC-CNN and NEP [14, 15]. The automatic cell segmentation in histopathological data set via two-staged superpixel-based algorithms has been studied in [16]. On the other hand, in artificial neural network they are image classification, partial information retrieval, incremental learning, focusing attention or learning regions of interests (ROI), and etc. Deep learning is the improved version of artificial neural networks technique that helps to find the optimal representation of data with non-linear methodology conventional machine learning method. Deep learning (DL) has found many techniques in signal and image processing and computer vision tasks such as character, pattern recognition, text generation and speech recognition, content-based image retrieval, feature extraction and classification. Especially, development in graphical processing units (GPUs) has boosted deep learning studies in academia and private sector [17].

Nowadays, diverse models based on deep learning have been successfully used on histopathological images and diagnostics, in other words, they use the computer-aided diagnosis (CAD) based on deep learning studies as mentioned in [18]. DL represents a highly promising subject for researchers dealing with histopathological images. In addition to that, computerized methods used in clinical works by pathologists and radiologists are utilized for detection and classification of cancer diseases which is called a second opinion and making the final decisions about cancer diagnosis. Today, the developments achieved in software algorithms and hardware techniques in the biomedical field has led large-scale researches on histopathological image analysis by using supervised [19] or unsupervised [20] machine learning algorithms. Several studies are underway on nuclei segmentation, object or anomaly detection and nuclei classification which are classifying the object into different groups and subgroups in consideration of their similarities in colors or textures. The most common algorithms for feature extraction and classification have been proposed and successfully applied in this area; for example, support vector machines (SVM) [21], K nearest neighbors (k-NN) [22], kernel Principal component analysis (PCA), Linear Discriminant Analysis (LDA) and etc. In image classification, one of the most important steps is the feature extraction. The overview of texture feature extraction techniques and the comparison between all these feature techniques which include Tamura features, steerable pyramid, and wavelet transform, Gabor wavelet transform were proposed in [23]. The SVM with two different classification schemes are used for object classification with various window sizes information in [24]. The classification based on CNN feature extraction with fully connected layer and support vector machine for classifying identified sub-classes were also proposed in [25].

1.2 Objective of The Thesis

In image analyzing process, diagnosis of cells can sometimes be mistaken due to so many signs that can often be shared with other cells in the related image. This reasons led to, doctors and professionals get it wrong in the diagnosis of the cell of cancer. Nowadays, the problem of cancer cells misdiagnosis is quite common and known to be on the rise in the pathologists field. So the main question here how we can handle a cancer cells misdiagnosis?.

In order to answer this question, cell structure is needed for overcome difficulty distribution of cells in tissue. In many cases the cells are surrounded by clutter represented by complex histological structures, for example: capillaries, adipocytes, collagen ..etc. The main goal of the first approach in our study, is to solve the complexity of diagnosis tissues in pathologists to avoid misdiagnosis of cancers cells, by detect the center of nuclei in the given images. Leads to obtain more information of cell structure in tissues, the research approach in chapter (3), is used fuzzy c means algorithm (FCM) clustering method which is extracted the foreground from background cellular structure of histopathological images, to obtain more details increase the ability of detecting the center of nuclei with using the automated center detection by using convolutional neural networks in two different sizes of histopathological data sets images which are (UCSB 200×200 pixels) and (CRC 500×500 pixels).

The motivation of the first approach of this study, we combined unsupervised method and supervised method for center nuclei detecting in order to obtain quite observe characteristic of the cell structure in tissues of histopathological images. On another hand, the second approach of this study, is the classification of nuclei in histopathological images, the feature extraction based on automated method of convolutional neural networks (CNNs) along with support vector machine approach is proposed to classify nuclei in histopathological images, into four different types of nuclei (i.e., epithelial, fibroblast, inflammatory and others) in a given data set. Furthermore, local phase quantization (LPQ) based feature extraction method is used to be able to apply it for classifying approach on the large size of data set images.

1.3 Hypothesis

In this study we attempted to use the coordination information (x,y) of cell, using for extracting more information of cell structure. In order to obtain details of tissues helped for quantitative diagnosis in pathologists. The aim of this study, foxed to find the center of nuclei in histopathological images, for solving complexity in diagnosis and solve the misdiagnosis of cells in tissues to obtain the actual cells in the related image contain. In recent years, many persons lost a life because of, wrong taken of cells or misdiagnosis cells, which is led to incorrect diagnosis of cancers in the tissue. Our contribution in this study, we attempted to use the coordination information of nuclei to help us finding a correct location of nuclei in related image contact. In the first data set for University of Santa Barbara (UCSB), we create a new data set coordination data set based on the ground truth information accompanied with the data set. The novelty of the first approach in this study, using the fuzzy c means method (FCM) with Convolutional neural network (CNN) in order to use it as a mask segmentation to obtain accurate diagnosis of cell or non cell in histopathological images. In the second approach in this study, we proposed a classification method to classify four cells of nuclei in histopathological images based on local phase quantization (LPQ) and convolutional neural network (CNN) classified by support vector machine (SVM).

2
General Information

In the chapter two, we described a brief exploration of general machine learning filed. Beside that, we proposed the theoretical background is important for understanding the methods discussed in the next chapter. We started to explain the related history of this area, machine learning, neural networks, deep learning, convolutional neural network and computer vision. In this chapter, we'll have to be more clear about what we mean by each of the involved terms.

2.1 Machine Learning (ML)

Machine learning proposed in [26] is the subfield of computer science. Machine learning algorithms are commonly used in computer vision applications, also these kinds of algorithms have different examples such as: Identifying object in images, transcribing speech into text and etc. The foundation concept of machine learning can be defined as a set of statistical tools that estimate complicated functions by learning from data. More details of computational learning in (ML) can be illustrated as given in [27]. "A computer software is a way to learn from experience (E) with represent to some class of tasks (T) and performance action (P), if its performance at tasks in (T), as can be measured by (P), improves with experience E." In the task (T) there is the first step which is started to learn the goal of the algorithm. That is defined by the user and in a usual way; transmission to the algorithms depends on providing an example of how an event can be processed. In this case, event means a set of features;

here event means a set of features characterize a single data point. That is usually called as the vector $x \epsilon R_n$ with entries x_i standing as features of the event. In Machine learning algorithms performance are usually trained on a set of X examples $x1, ..., x_N$, denoted to as the training input set, with an output mapping $f(x)$. Afterwards, a quantitative measure is processed to assess how well the method performs. In a usual way, performance measures are accuracy, i.e. proportion of correctly mapped samples, and error rate; it is a proportion of samples for which the method has produced the

7 wrong outputs. Also, numerous measures exist and the choice of performance measures is often task-dependent. In order to allow an unbiased assessment of the algorithm, it is crucial that the model is assessed on an unlabeled data set that can be referred to as the test set. The performance measure (P) is the metric by which the competence of the algorithm is evaluated. In a usual way, the metric is chosen by the user. In the case of detection and classification algorithms, in performance measure P, it can be employed a loss function that quantifies the disagreement between the predicted and true output information. The simple case of the loss function could be the amount of correctly object events in proportion to the total number of events. In more sophisticated approaches, it is a continuous-valued score for each event. In a case of performance it is tested on data that were not included in the training sample. This independent sample is called the validation data set or validation sample. In order to estimate how well the algorithm will perform in a broader range of methods, additional performance tests not related to the chosen loss function are performed. In experience E, the provided data set and any other information which the machine learning algorithm provided can be used to learn. Here the supervised and unsupervised algorithms can be differed. These algorithms are not quite exclusive and applications can be combined both methods, named semi-supervised learning. That it is still a promising paradigm to solve different machine learning goals. All these algorithms can be represented as a research area and can be defined as shown below: Supervised learning method, Unsupervised learning, and Semi-supervised learning and Reinforcement learning.

2.1.1 Types of machine learning

Supervised learning

In machine learning models most of researchers are used supervised learning [28] methods that is input a data set of labeled data while training an algorithm. In order to compare its actual output with the training examples, for predicting correct label outputs. The machine processes after that, modifies its internal adjustable parameters to reduce errors and estimate the right answer.

Unsupervised learning

The second type of machine learning is unsupervised learning, this algorithm processes data without label and finds patterns; the concept of this method is to have the computer based learning and how to predict something that we don't tell the model to do [29].

In the unsupervised learning the goal is to find structure to the input data. We can refer the unsupervised learning types as:

• Clustering method which is a set of unlabeled data to be divided into clusters, such as: K-means, or fuzzy c means.

• Amontly density estimation is finding the distribution for the inputs in some space.

• Dimensionality reduction algorithms that are commonly used in unsupervised learning such as: Principal component analysis (PCA), independent component analysis (ICA) or autoencoder. In these algorithms the main concept is to find the best representation of the data with fewer dimensions. Semi-supervised learning can be defined as learning between supervised and unsupervised learning problems. Here is where it deals with partially labeled data sets.

Semi-supervised learning

Semi-supervised learning can be defined as learning between supervised and unsupervised learning problems. Here is where it deals with partially labeled data sets. That can be costly and time-consuming to obtain labeled data sets which are often limited in size, in contrast to often large unlabeled data sets that are freely available. However, the aim of semi supervised learning is to supplement the limited labeled data with unlabeled data in order to improve learning [30].

Reinforcement learning

Reinforcement learning: One of type of machine learning algorithms, in reinforcement learning methods that is trying to find the best ways for learning. For more knowledge, reinforcement learning is proposed in [31].

2.1.2 Conventional artificial neural network (ANN)

Traditional machine learning algorithms are linear [32]. Neural networks are a common linear model in machine learning algorithms [33]. It can be described as an information processing model inspired by the brain's structure. Neural networks in some cases are modeled as distinct layers of neurons, named hidden layers. The basic unit in neural networks is a neuron, it is also, named as node or unit. The process is started to receive the input element source from neurons in the immediately preceding layer, the value will be processed and propagated forward through the network layer by layer, in order to, provide the final output layer. Besides, after processing and taking features to feed it to another hidden layers, it can be called a feed-forward process

[34]. In Fig. 2.1. We can see the basic scenario of neuron in artificial neural network. The output $y_n = v_n(\sum_{n=1}^{m} w_{mn}x_m)$. Where v_n represent as activation function, weight in this equation denoted as w_{mn} and the input parameter denoted as x_m as shown in figure 2.1.

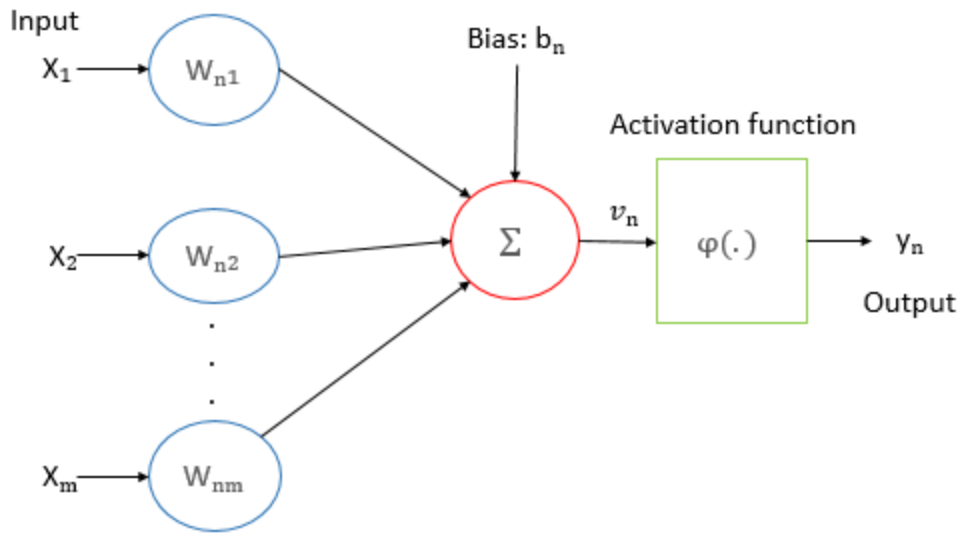

Figure 2.1 Basic scenario of neuron in artificial neural network

Finally, the output of these processes can be compared with the training data with an error function and evaluation which is applied in the output layer in order to help a network for a better prediction.

Activation function types

Activation function types most of the investigators in neural network methods using a sigmoid, tanh or rectifier linear unit (ReLU), they function in nonlinearity functions which are a complex function. The activation function used for calculating the weighted sum and then it added the bias in the neuron of the network and made a decision if it should send it or not. If we consider the output of the neurons as:

$$k = \sum(W \times X) + b \tag{2.1}$$

Here in equation 2.1, w is the weight score, X is the input elements with b is referring to bias.

• ReLU

In most of the neural networks in the past few decades, the nonlinear activation function is used, which is called Rectified Linear Unit (Relu). The most of commonly used in an activation function in deep learning methods are the Rectified Linear Unit (ReLU). ReLU is an activation function produced by [35].

• Sigmoid

Applying of sigmoid as shown in fig 2.2 logistic activation function outputs were re-scaled between (0, 1). The probability distribution over a binary variable can be used by the sigmoid function as stand as below in 2.2:

$$\sigma(a) = \frac{1}{1 + e^{-a}} \tag{2.2}$$

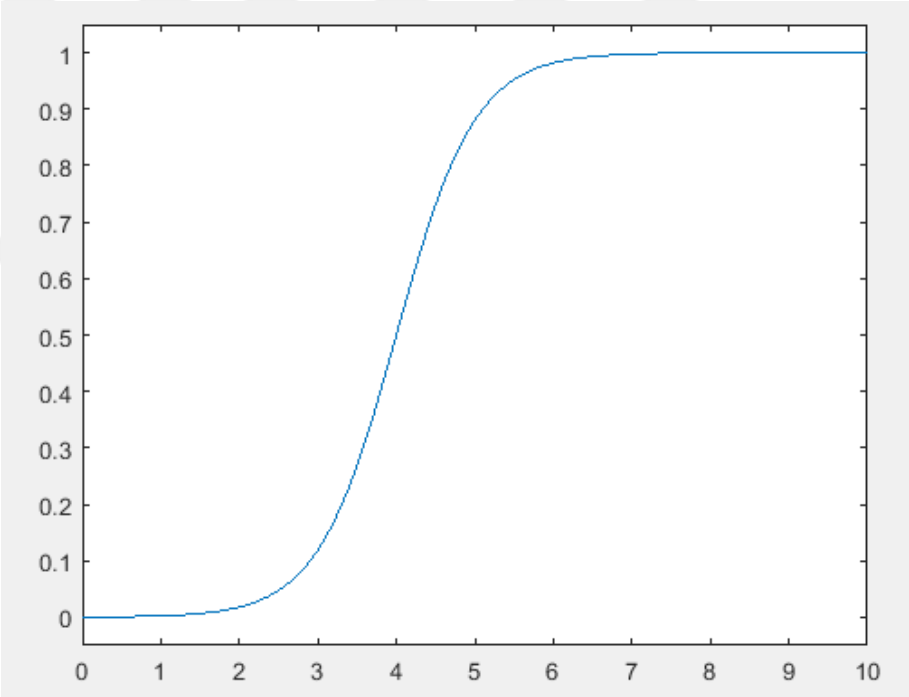

Figure 2.2 The sigmoid function

• Tanh

Activation function, using the tanh as shown in fig 2.3 function as we can see in equation 2.3 output, the rescale can be between (-1, 1).

$$f(k) = tanh(k) = \frac{2}{(1 + e^{-2k})} \tag{2.3}$$

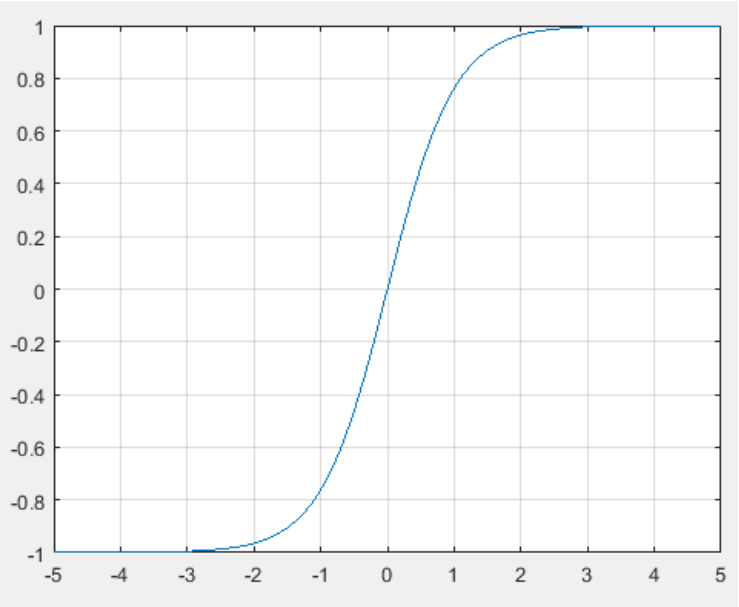

Figure 2.3 The tanh function

2.1.3 Deep learning

Deep learning is the concept of artificial neural networks and computational systems that acted the functions of the human brain. The history of starting deep learning, it is back to 1943 when Warren McCulloch and Walter Pitts formed a combined model for neural networks based on algorithms of neural logic and algorithms. In late 1940, psychologist Donald Hebb created a learning hypothesis based on the mechanism of neural plasticity, which is known as Hebbian learning. In his work, Hebb, who uses the neuron of the cell, explored the interactions between two neurons of cells, and his rules based on the fundamental of neural networks [36]. This learning has been recognized as a 'typical' unsupervised learning rule. In 1958 using simple addition and subtraction operations proposed by [37] it is created, perceptron which is a supervised pattern recognition algorithm based on artificial neural network [38]. models with activation function of complex equations is used in [39] in their work, the cybernetics Prediction tools is proposed to develop deep learning algorithms. The backpropagation algorithm developed by [40] which is effectively solved the XOR problem, the backpropagation algorithm is developed the deep learning field. In 1988, it is suggested by [41], and a hierarchical and multilayered neural network used for handwriting recognition and other pattern recognition problems. In this design, the learning process of the computer is done using visual patterns: In 1989 convolutional neural networks with Backpropagation network for data analysis by [42] the development of deep learning is proposed a recurrent neural network was proposed by [43] to solve long-term dependence problems of (Long Short Term Memory) LSTM [44]. In mid of 2000th, a study by "Deep Learning" began to gain popularity. However, it has

been shown how a multilayer neural network can pre-train a layer at once. The Hinton lab assists to solve the training problem for Deep Neural Networks [45]. The performance of artificial pattern recognition algorithms, which consists of over 16,000 processors and over one billion connections, has reached the human level by Google's research team in 2012 [46]. Also, AlexNet architecture proposed by Alex Krizhevesky in 2012. Recently, deep learning architectures have used in different research area, when they have outstanding performance in variance computer vision and pattern recognition tasks [47–50]. Convolutional neural networks have been especially successful in several complex problems. proposed LeNet, it is used to read zip codes, digits, etc. AlexNet represent as the next notable CNN used in computer vision, that has a very similar architecture to LeNet. However. it has a large numbers of layers and parameters. Notably, a breakthrough in AlexNet is that multiple convolutional layers in AlexNet were stacked on top of each other whereas LeNet architectures included only a single convolutional layer. VGGNet [51] used that for the task of image classification, deeper networks generally have a good implemented. There were sixteen convolution and fully-connected layers in their best performing network. GoogleNet [52] proposed the concept of an inception module which is dramatically reduces the number of parameters in the network. Besides that, rather that using fully-connected layers as in the upper layers of CNN, it uses average pooling to decrease a large number of parameters. Network depth is crucial in neural network architectures. Intuitively, deeper networks should perform no worse than their shallower counterparts. However, very deep networks degrade in performance. To address this issue, ResNet [53] bypassed signal from one layer to next via adding a shortcut connections with identity mapping, Wide residual network [54] reduced depth and increased width of residual networks, and ResNeXt [55] computed a set of transformations with the same model.

2.1.4 Convolutional neural networks (CNNs) general description

Convolutinal neural networks (CNNs) is a deep learning based algorithm proposed by Lecun et al. To classify handwriting digit images [56]. CNN is consisted of three main sets of layers: convolutional layer, pooling layer and output layer. Network layers are compatible in a feed-forward, back-propagation neural networks construction: each layer of justification is followed by a pooling layer, and the last part of this layer is followed by the output layer with feature maps. The convolution and pooling layers are represented as two-dimensions layers, while the output layer is considered as a 1-D layer. In convolutional neural network, each 2 dimension layer has several levels. In one level it can observe neurons that are arranged in a 2-D array. Also, with respective of the output layer we can obtain a feature map each convolutional layer can produce

a feature map Fig 2.4.

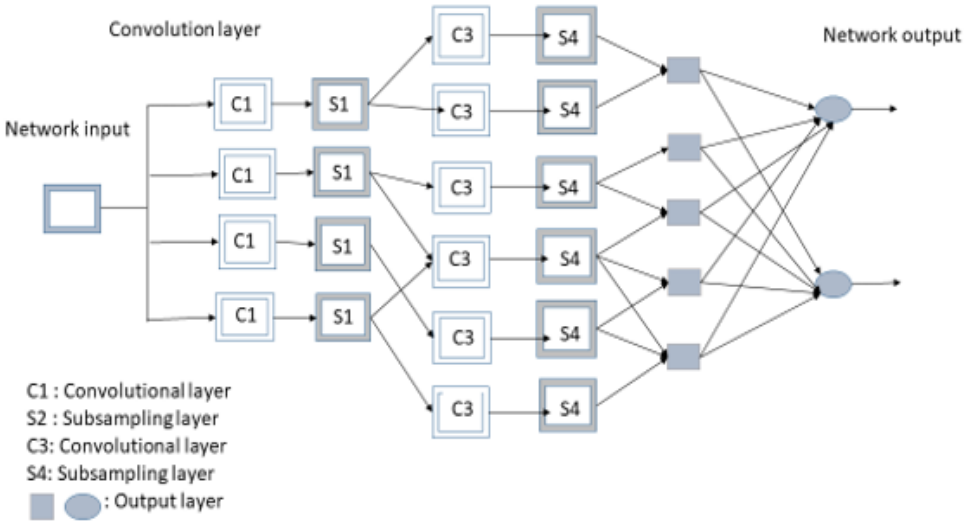

Figure 2.4 The output feature map of CNNs

In a convolutional layer as shown in Fig. 2.5, each layer is linked to one feature maps or more of the next layer. This connection is adjust together with a convolution mask, that is a two-dimensional matrix of adaptable entries weights term. The convolution output parameters can be collected as shown in Eq. 2.4: Where weight and bias are added to compute the output of this layer in order to produce feature map.

$$k_n{}^l = f_l(\sum_{i \in v_n^l} k_i{}^{(l-1)} \otimes w_{i,n}^1 + b_n{}^l) \tag{2.4}$$

where l stands as a layer for neurons of network, f_l denoted as an activation function, $k_n{}^l$ is represent as feature map the output parameters. Also, $H^{(l-1)} \times W^{(l-1)}$ is represented as a pixels size of convolution mask in this equation $H^{(l-1)-r_l+1} \times W^{(l-1)-c_l+1}$, with $\otimes$ as 2D convolution operator v_n^l represents list of levels in layers l-1.

Pooling layer as will show in Fig. 2.6 is applied to decrease the size of the feature map for further analysis in the next layers. As an example, the sum of four pixels is calculated and multiplied with weight before it is added to bias term. Then the result is sent to the activation function to obtain an output for the 2×2 block. At the end, each pooling level minimizes its input size into half, along each dimension. A feature map in this layer is connected to one or more level, then it must be connected with next convolution layer feature map for this layer obtained by Eq. 2.5:

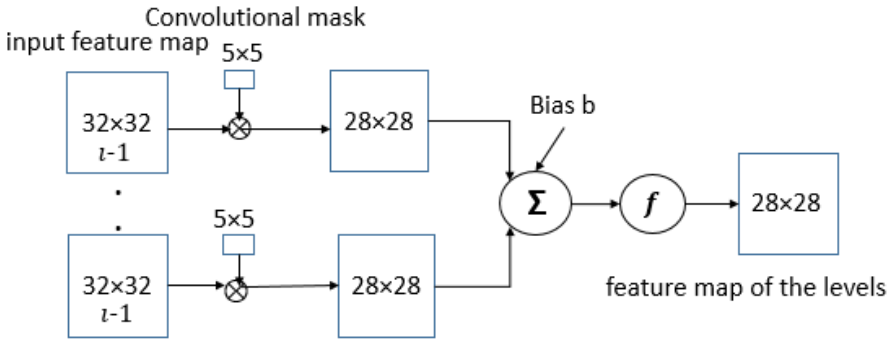

Figure 2.5 The convolution layer in CNNs

$$k_n^l = f_l(z_n^{(l-1)} \times {w_n}^l + {b_n}^l) \tag{2.5}$$

where, the feature map n is divided into blocks each of them consist of 4 pixels (2×2) in layer (l-1), where $z_n^{(l-1)}$ is a matrix of that result concluded from the four pixels in $(l-1)$. In the last convolution layer, each level in this layer connected to one of feature maps and convolution masks which have the exact same size as its input feature maps as proposed in [57, 58].

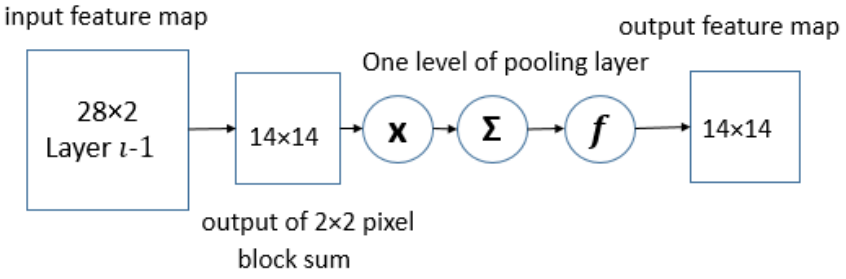

Figure 2.6 The pooling layer in CNNs

The last part in CNN algorithm is commonly called as fully connected layers. The construction of this layer is started with connecting the high level features extracted from the last previous layers to the classification part. The outputs are based on a probability value from zero to one for each of the classification part. In this instance, the number of classification types must be the same as the numbers of output in the CNN algorithm.

$$k_n^l = f^l(\sum_{m=1}^{N^{L-1}} k_m^{L-1} w_{m,n}^L + {b_n}^L) \tag{2.6}$$

$$k = [k_1^L, k_2^L, k-3^L ..., k_{N_L}^L] \tag{2.7}$$

where L denoted the output layer; N^L is the number of output; $w_{m,n}^L$ stands as the weight and (m,n) are the size of pixel of the last convolutional layer as shown in Eq. 2.6. The bias term ${b_n}^L$ is denoted as the associated with n neuron of layer L. The calculation of neuron outputs can be presented as in Eq. 2.7.

Data augmentation and regularization, neural networks models it needs to add more information to the loss function that helps to use penalty on the certain types of weights, also this strategy is used to protect against overlearning and to decrease the generalization (test error). Besides that, sharing parameters features of convolutional networks can be represented as an example of regularization. Several techniques are used as a regularization way for example dropout [59]. Commonly, in (CNNs) the dropout method is used in the last fully-connected layers. Overfitting processes also is the option to apply by increasing the amount of training data in the models. Data augmentation is used to generate more actual samples from the input data set. For classication methods using convolutional networks, we can increase the data set training by flipped images, rotated or crops and scales. Also, in same studies noise can be added to the input data set images to increase images in data set.

2.2 Computer Vision

Computer vision is one of the automation which allows the perception of machine vision and development of computer vision systems to find the information of image and process it in the same way that human vision does [60]. The development in the computer vision methods has produced new tasks to this area of machine learning, include, learning which is received from structured details, image classification, progressive learning, focusing attention, learning regions of interests (ROI), and also learning with multiple classes, etc. Difficulty in this fields which it will happened in the development of new, more robust machine learning approaches that will be able to work in more realistic performance.

2.2.1 Object detection and classification

Object detection and classification: The definition of object detection is to set the location of the object in related images that we can identify this process as an (object localization), also the affiliation of each class denoted (object classification) [61]. The traditional scenarios consist of three models which are feature selection [62], feature extraction [63], feature extraction [63], and classification. The feature selection processes work to choose variables which are appeared in a given image that has different sizes or ratios. Feature extraction aims to extract useful and visual features and characteristics from the input data sets. In this case we need to extracted visual features to recognize object, HOG [64], SIFT (scale invariant feature transform) [65], Haar-like [66] are provides feature helps to linked with complex cells in pathological images [67]. However, due to the clutter problems and backgrounds complexity, it's difficult to manually design a robust model for feature description to perfectly describe all types of objects. Classification is needed to recognize the object categories based on statistical classifiers (e. g. Neural Networks [68], Support vector machine (SVM)[69], Adaboost [70], Deformable Part-based Model (DPM) [71], etc) were introduced. Object detection methods are the most activated challenging tasks in computer vision, they are helpful to highlight the most central object regions in the related images. The area in object detection has several applications for example robotics, medical image analysis, surveillance, and human-computer interaction. Today, the object detection methods are designed intelligently well to constrain domains, and use quite sensitive ways to clutter and occlusion issues. The detection of the objects of the specific class of the related images needs to have some information such as the object position and the image in which it is segmented the object. In classical object detection algorithms, there are handcrafted features and oversimplified trainable architectures. In this way, the performance of these methods is easily inclined by constructing complex ensembles that combine multiple low-level image features of a high-level context of object detectors and scene classifiers. In recent years, the increasing development in deep learning approaches leads learning the high-level and the deeper features that are introduced to reveal the existing problems in classical architectures. These scenarios act differently in a network structure, training strategy and optimization function. The basic idea that says most of the object detection approaches has considered the same main scheme is known as a sliding window process. That is to detect the object spearing in the image of different levels and locations, the basic point of the object detector indicates if a given image patch is matched to the object or not. Where the classifier simply works at a given level and image size, the different versions of the input image are generated at various levels, and the classifier is used to classify all possible images of the given size, for each of the down scaled type of the image. In addition, more information of combining sparse region with (CNN) is proposed [72].

3
Detection of Nuclei in Histopathological Images

3.1 Detection of Nuclei

The identification of initial signs points, of one per nuclei and near a position to its center is stands as the essential and important for most nuclei segmentation models [20]. Nuclei detection approach consist of two methods the first method is a clustering method fuzzy c means (FCM), clustering algorithm consists of two ways (automatic, semi-automatic) and convolutional neural networks (CNN) together aims to detect the center of nuclei. Nuclei center in this method is detected by the mask of nuclei consist of combining fuzzy c means algorithm along with convolutional neural networks (CNN).

In medical image technology, it becomes possible to obtain more meaningful information by applying pre-processing of pathological images. In recent years, the development which happens in deep learning architectures, had increased quality of data analysis for more information related about the image content. In this approach of this study we can answer three questions, led to solving cell structure issues in pathologists diagnosis or in other word misdiagnosis cells in tissues structures.

Question (1) Why we need automated algorithms for finding cell structure information, and why we need cell structure information in histopathological images?

Question (2) How the automated methods impacted in this work to detect nuclei cell structure information in histopathological images?

Question (3) How we are going to find the center of nuclei in histopathological images?

According to question one, we can say that we need an automated method for quantitative diagnosis of tissue. And also, we need cell structure for overcome difficulty distribution of cells in a tissue, automated method for cell structure is needed in regularities of cell shapes. Also, the answer to the second question, it is reducing the consumed time in the analysis of cells in histopathological images, whereas, in the conventional manual methods is relatively time-consuming work for pathologists. In addition, cell count in tissue has significance in the diagnostic of cell or no cell. Solving the complexity in cell structure, in many cases, the cells are surrounded by clutter represented by complex histological structures, for example, capillaries, adipocytes, collagen, etc. In this work, we obtained the coordination (X, Y) information and used it to extract the actual cells and the wrong sharing cells with the actual cells in the diagnosis of the cell structure in histopathological images. According to the last question, we can answer it by tracking methodology of this chapter of this study.

This approach in this work includes detection the center of nuclei via two different techniques depend on the coordination (x,y) ground truth image information. First technique, We use clustering method fuzzy c means algorithm, for discriminating the background pixels from the foreground pixels which contains the region of interest in order to, detect the center of nuclei from the images are obtained. Second technique, tiny convolutional neural network (Tiny-CNN) is used, for detecting the center of nuclei on two different size of pathological images .

3.2 Experimental Data Set

The first experimental data set (UCSB-58) is obtained from David Rimm Laboratory in Department of Pathology at Yale University of California, Santa Barbara. The data set is selected from a part of UCSB biosegmentation benchmark and includes 58 set of histopathological images 200×200 size of pixels consist of 32 benign and 26 malignant tissue images [73]. The size of pixel in this images is 896×768. Additionally, each of this UCSB-58 data set images is corrupted labeled by pathologists to become 200×200 pixels images with ground truth as shown in Fig. 3.1.

In addition of that, we create coordination (X,Y) ground truth Information on (UCSB) data set, image size (200 x 200), based on the nuclei ground truth information accompanied with (UCSB) data set. We selected manually on the (x,y) points based on the real information of the ground truth information. In order to produced a new coordination data set for (UCSB) data set images as we can shown in Fig.3.2.

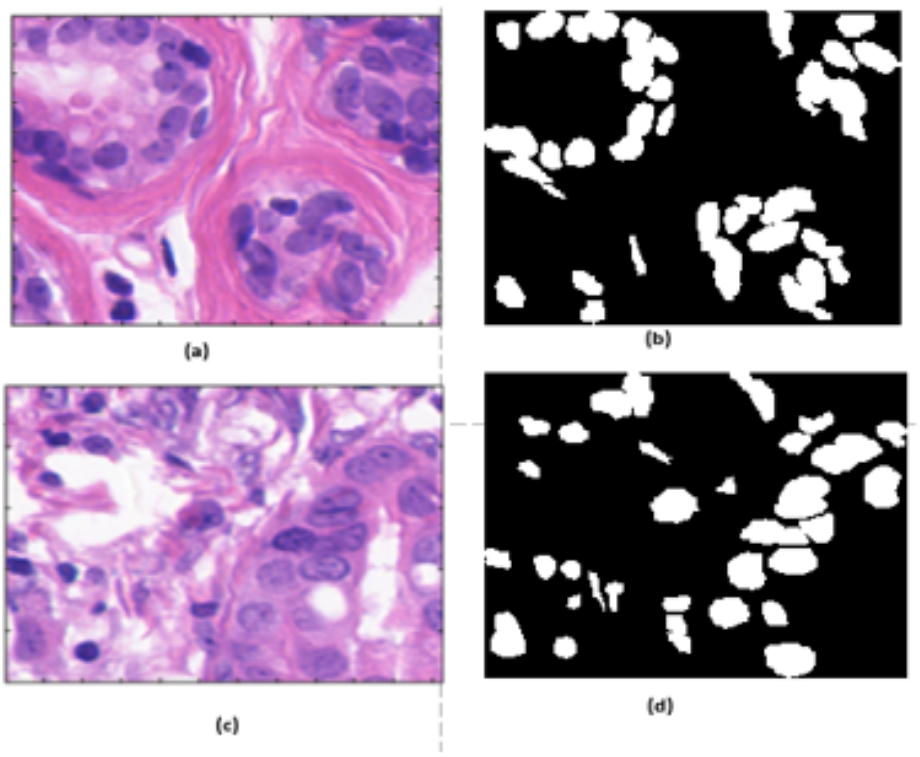

Figure 3.1 Data set (a) original image, (b) ground truth image (a), (c) original image, (d) ground truth image (d)

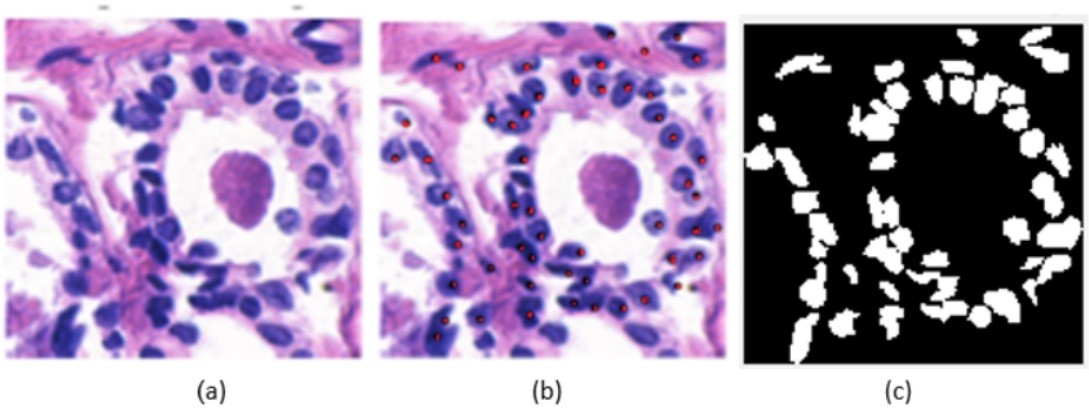

Figure 3.2 (a) original image (UCSB- data set), (b) (x,y) data set (c) original ground truth image

The second data set (CRC-100) is obtained from Department of Computer Science at University of Warwick [15]. This study involves all the 10 $E\&H$ stained histopathological slide images in size of 500 × 500 at a resolution of 0.55μ m/pixel (20 × $optical$ magnification). For detection purposes 29756 nuclei are signed at the center as shown in Fig. 3.3 and out of 22444 nuclei centers have an associated class label for classification purpose.

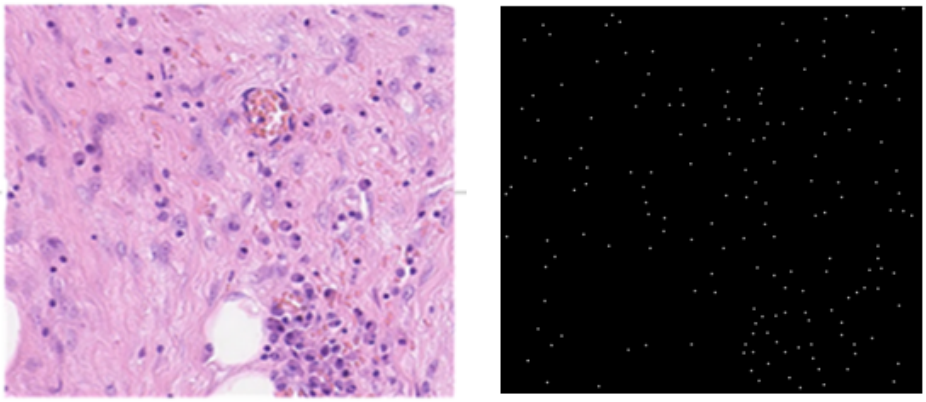

Figure 3.3 (a) original image (CRC- data set), (b) (x,y) data set

3.3 Fuzzy C-means Clustering Algorithm

Clustering is a method of locating a set of values into group. In this instance, the clustering methods can be classified into several classes: hard clustering and soft (fuzzy) clustering. One is hard clustering; second one is soft clustering. In this study, a soft clustering method, fuzzy c-means, is applied to find the cellular structures in histopathological images. Soft clustering FCM in many cases more resilient than other hard clustering method. In soft clustering, elements belongs to more than one cluster, and connected with each element is set of membership levels as mentioned in [74]. This method is first proposed by Dunn in 1973 [75] and developed by Bezdek in 1981 [76]. In the nature work of FCM algorithm is depend on assigning membership for each class, in this algorithm the class number should be greater than 1 and less than the number of N pixels in the input image X.

$$J_m = \sum_{i=1}^{N}\sum_{j=1}^{c} u_{ij}^{m}||X_i - C_j||^2 \tag{3.1}$$

Here, the Eq. 3.1 illustrated u_{ij}^{m} is the degree of membership of x input image in the

J denoted as a cluster m represent to any real number grater than 1, and the last term $||X_i - C_j||^2$ represent to a norm between any measured data and the center. The clustering centers calculated in FCM is shown in Eq. 3.2:

$$C_j = \frac{\sum_{j=1}^{n} u_{ij}^m x_i}{\sum_{j=1}^{n} u_{ij}^m} \tag{3.2}$$

where, j stands for each cluster center, x_i is the objects in j and u_{ij} is the degree of membership of x_i, the value u_{ij} is the degree of membership of x_i in cluster j.

The membership matrix of u_{ij} is calculated by using d_{ij} as follows in equation 3.3.

$$u_{ij} = \frac{1}{\sum_{k=1}^{c} \left(\frac{d_{ij}}{d_{kj}}\right)^{2/m-1}} \tag{3.3}$$

The iteration in this algorithm is stop when the $||u_{ij}^{t+1} - u_{ij}^t|| < \varepsilon$ which is denoted as a termination criterion between zero and one. t in this term represent to the iteration steps.

The simple brief steps of fuzzy c means algorithm are mentioned as we can see below:

1- Specify ε, m,c.

2- Initially, the U_{ij} membership matrix is generated at random, with fuzzy m.

3- Centers are determined as we proposed in equation 3.1.

4- The distance between the any data and centers for each pixel is calculated.

5- The current matrix u_{ij}^{t+1} is updated.

6- Check the stopping criteria, the difference between the membership matrix in the previous step and the updated membership matrix.

7- The same procedure is repeated from Step (3) if it is above the specified threshold, the cluster center is calculated again.

3.4 Nuclei Detection in Histopathological Images via Fuzzy C Means Clustering Method and Convolutional Neural Network.

In this section of this study, we propose a new way of combining method and evaluate two machine learning algorithms, which are supervised method using convolutional neural network and unsupervised method using fuzzy c means (FCM) algorithm as automatic approach detect the center of nuclei using the stander deviation (STD) of the pixel intensity in the histopathological images, and using fuzzy c means semi automatic approach. Which is select the closest cluster to detect the center of nuclei manual after clustering the regions in one image into five clusters. Afterward, the result of fuzzy c means semi automatic approach multiplied with the result of an automated method which is respect with tiny convolutional neural network (Tiny-CNN), to find the last image produced via combined these two methods together. The objective of this experiment is to detect all nuclei in an image by selecting their center positions, regardless of their type labels. In order to obtain more information of cell structure in pathologists images.

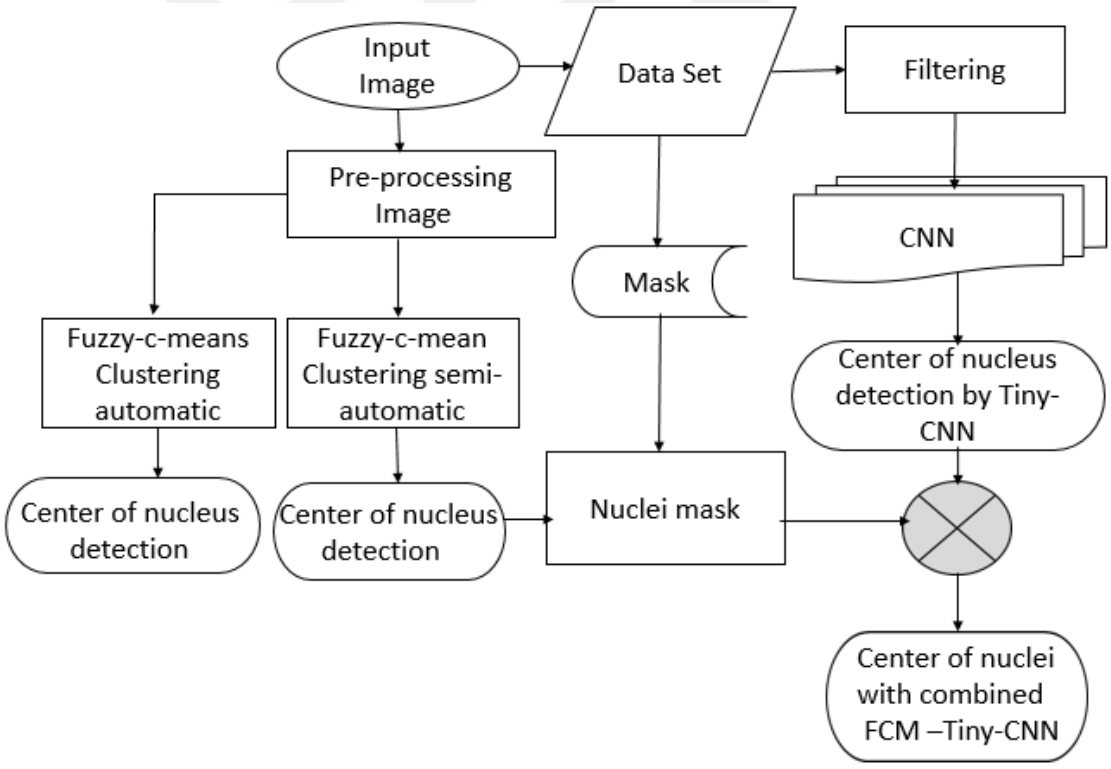

Figure 3.4 Flowchart proposed methodology

3.4.1 Nuclei center detection via fuzzy c-means clustering algorithm.

The fuzzy c means (FCM) clustering algorithm has assessed the performance of different algorithms for nuclei segmenting to extract the nuclei in the histopathological images. Two essential procedures are implemented in this part of study, the first one has segmented the nuclei and detected the center of nuclei automatically by using the standard deviation (STD) method, whereas the second one is applied flow the same scenario of automatic part, however, in this approach manual option is added, after calculated of (STD). After that sorted results for five clusters, the best cluster from five different regions of clusters is selected as shown in Fig. 3.5. This approach is called a semi-automatic approach in all sections of this study. In brief, we can explain these two algorithms as given below.

(Procedure (1) fuzzy c means automatic

• Load the data set in this study two different size of histopathological images are used as input data set, the first data set from the lab of University of Santa Barbara (UCSB 58-set), the second data set obtained from Department of Computer Science at University of Warwick (CRC -100 sets).

• Down scaling is applied it has implemented the gray scale after that, convert in to class double and put the image pixel intensity in to one column.

• Implemented the fuzzy c means for selected data in 5 clusters. The fuzzy c means algorithm is used to extract non-cells in the structure and detect the center of nuclei in histopathological images. The processes of clustering method have divided the data in the image into several clusters or groups in the proposed data set as it is shown in Fig. 3.5. In addition to that, the size of data in this processes M-by-N, which represented M as the number values and N as the number of coordinates for each data point. The (x,y) for each cluster center is yielded in the rows of the matrix center. Besides that, the matrix U has included the category of membership of each data point in each cluster and the value zero and one denoted as no membership and full membership respectively. The level between zero and one can be evidence that the data point has partial membership in the cluster and at each iteration, an objective function is increased to have the best location for the cluster and its values are yielded in the objective function.

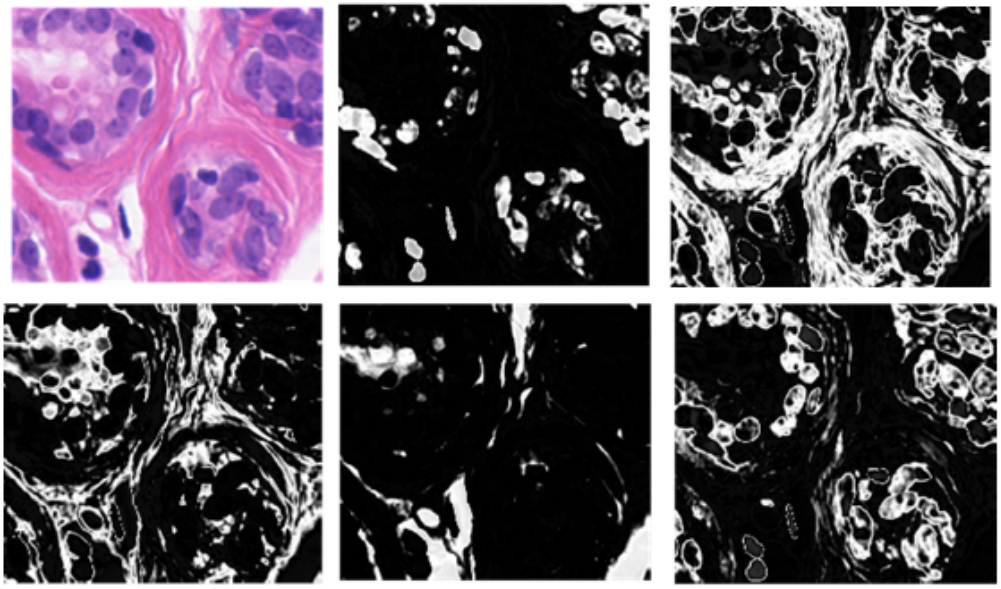

Figure 3.5 Regional outputs of five different clusters obtained by FCM algorithm

• Create a matrix and compute the maximum standard deviation of each column the result is shown in Fig. 3.6. In this case we noticed that the result one before maximum (STD) is better than the maximum one. After that standard deviation for each cluster is calculated, and select one before maximum one automatically.

• The segmentation step is applied by using Otsu's method based global image threshold for each image to find the threshold value for segmentation.

• Then a dilation morphological operation is applied to the result of segmentation. After that the binary image obtained from the Otsu's method is multiplied to the original image to eliminate the possibly non cellular structures. Binary dilation of A by B, indicated to $A \otimes B$ which is defined as:

$$A \otimes B = z|\widehat{(B)}_z \cap A \neq \phi \tag{3.4}$$

In this equation, $\widehat{(B)}$ represents a reflection of the structuring element called B . In other words, it is the group of pixel positions z, the reflection structuring element overlaps with foreground pixels in A when translated to z.

• Morphological operations are used on the proposed images by removing unwanted regions. Three sets of morphological operations are applied so as to remove the unwanted objects while retaining the desired objects.

• Applying mask using method divides the whole image into two regions, one for cell and one for non-cell regions. This helps in obtaining the contour which surrounds all the nuclei by separating the image using the values of the data points.

• The outputs obtained from the previous operations are combined with the original image to give the final mask in this algorithm as shown in Fig. 3.7.

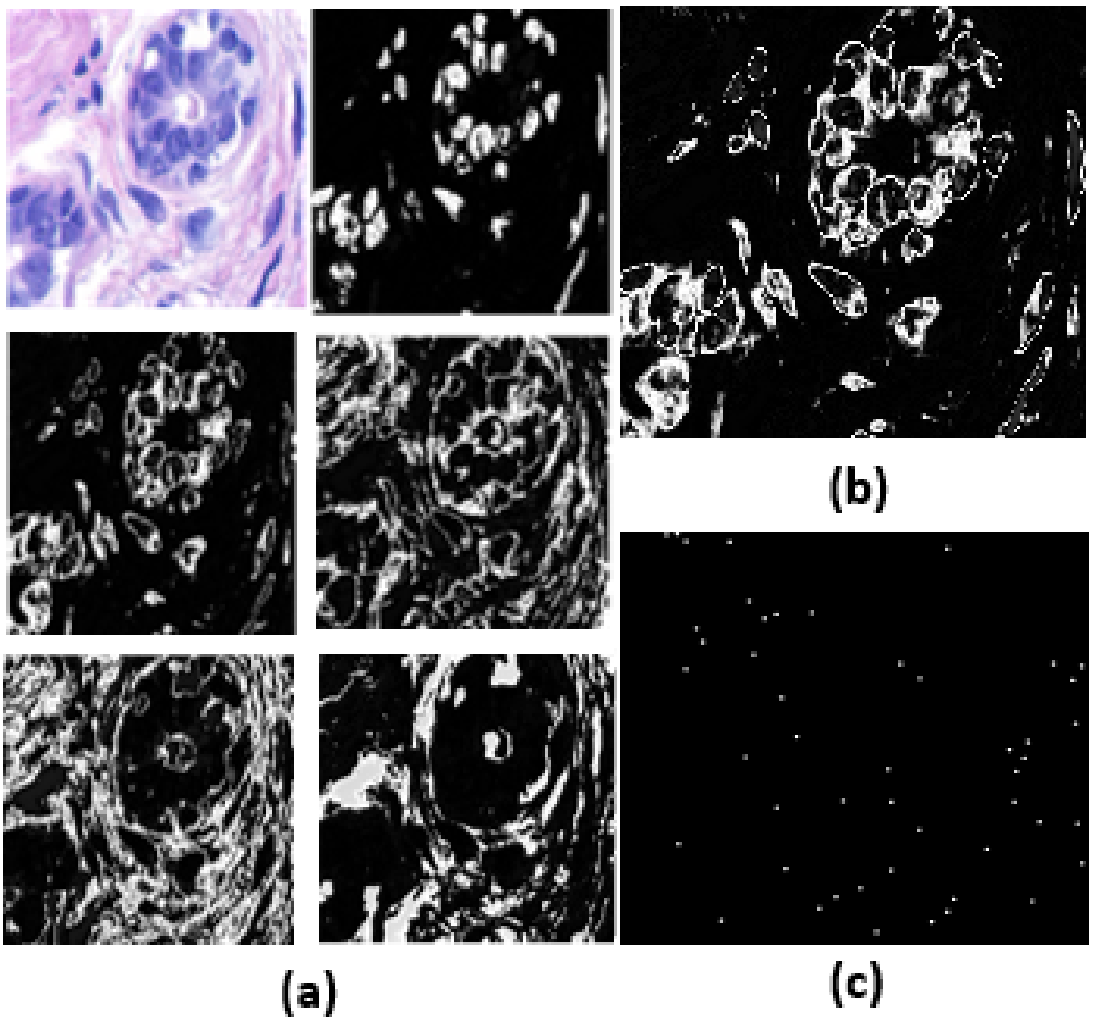

Figure 3.6 (a) Five different cluster regions of FCM algorithm (b) obtained nuclei cluster of FCM approach with maximum standard deviation and(c) final output nuclei centers image.

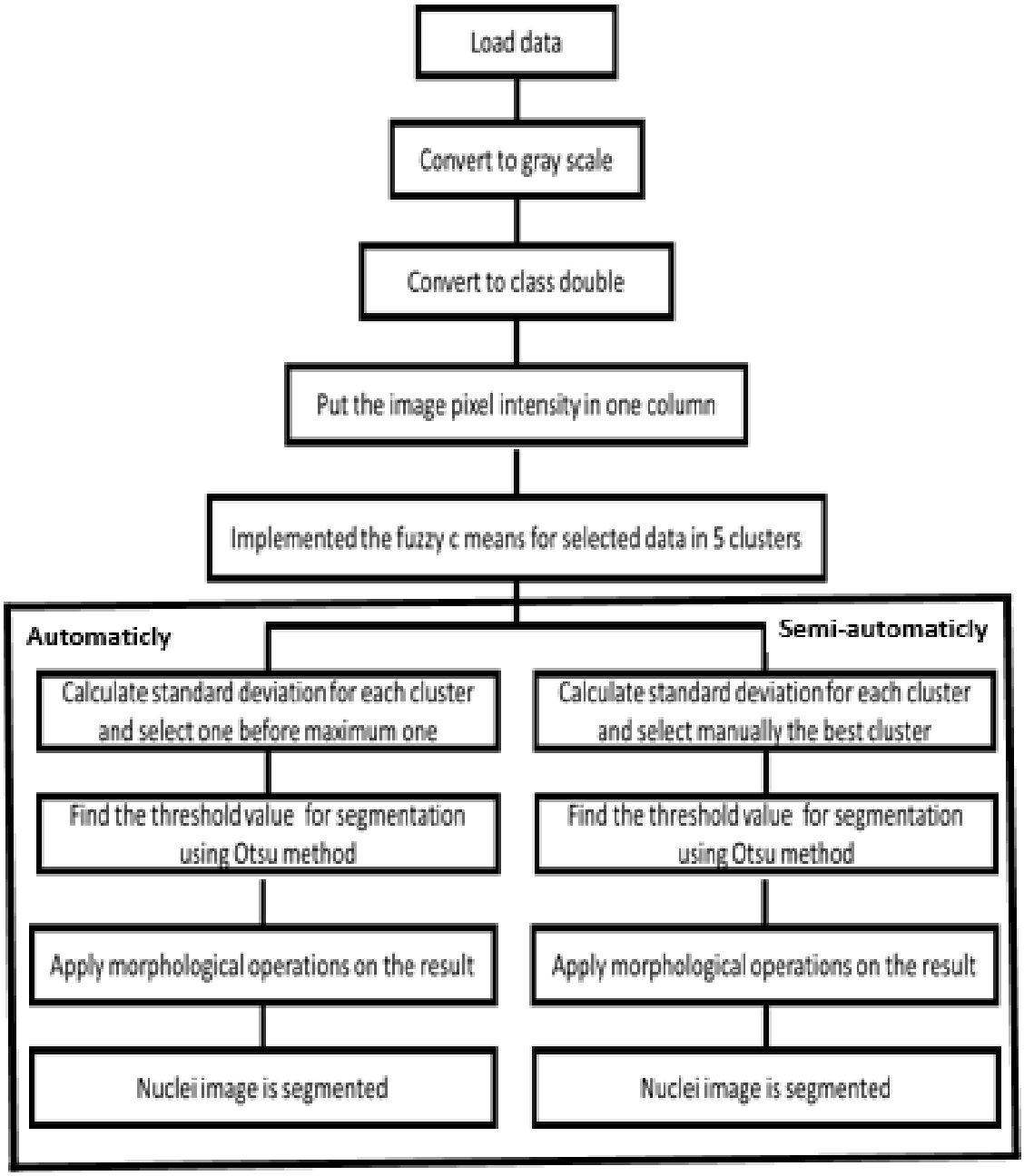

Figure 3.7 Sequence steps of fuzzy c means automatic and semi-automatic approaches for detecting the center of nuclei in histopathological images

Procedure (2) fuzzy c means semi-automatic

• The second approach of fuzzy c means (FCM) is called a semi-automatic algorithm. It can be describe it as the same as the previous steps of automatic approach, that based on sorted the result of each cluster and select maximum standard deviation cluster automatically. At the first experiment of this approach, we observe that the intensity value in each repeat of the algorithm most of time the cluster one before the maximum standard deviation is better than the maximum cluster, as shown in Fig. 3.8. Also, we find the opportunity to increase the result of cluster needs to add the manual option used for finding the best cluster which seems closest to the ground truth information of the given data set as shown in Fig. 3.7. In Fig. 3.9 is shown the center of nuclei in histopathological image has obtained via (semi-automatic) approach by select the nearest region from the five regions.

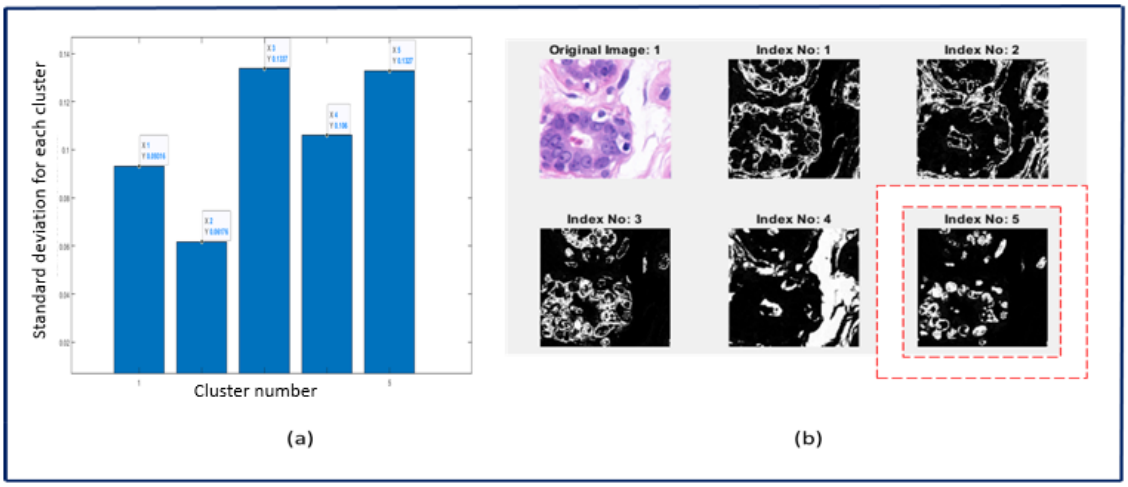

Figure 3.8 (a) Standard deviation results for each cluster illustrated the intensity value for each cluster (b) select the best cluster manually (semi-automatic)

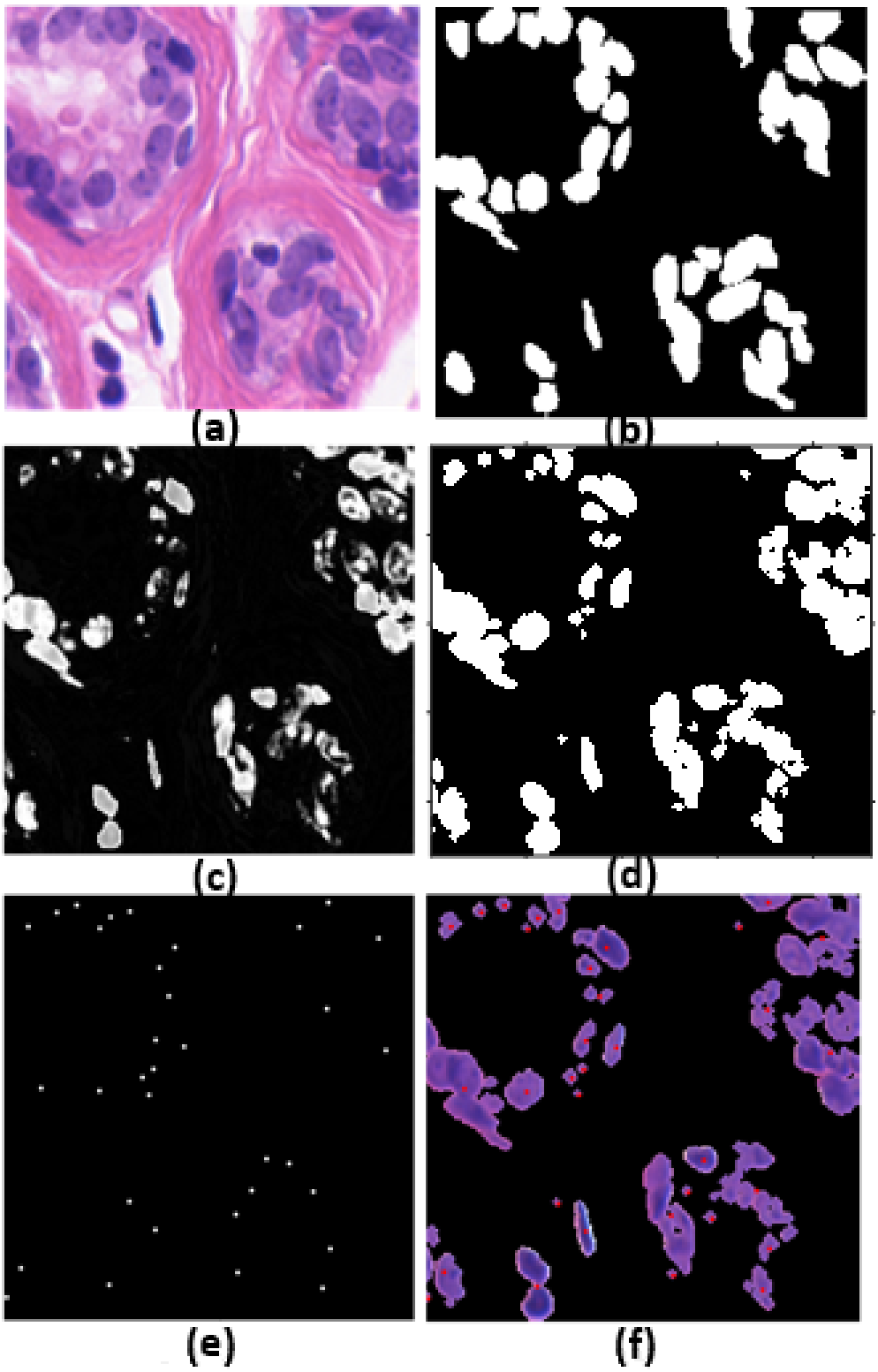

Figure 3.9 a) An original image from UCSB-58 data set, (b) its ground-truth, (c) FCM result after choosing closest cluster manually, d) FCM result after morphological operation, (e) FCM nuclei center detection and (f) masked image of nucleus with center detection

3.4.2 Experimental results obtained by fuzzy c means clustering method

Misdiagnosing of cell structure analysis is represented, one of the most problematic points in pathologists. The cellular structures of the high success of the correct cellular structures segmentation are very important to the detection of the regions of the actual cells in diagnosis. Fuzzy c means algorithm in this study have detected the center of nuclei based on the information of the coordination (x,y) in two histopathological data sets (UCSB 58 sets high resolution), and (CRC 100 sets), at the first experiment result for the first approach with maximum standard deviation we sort the result for each cluster and observed that the intensity value (x,y) in the cluster one before maximum standard deviation is better than the maximum one, in most of experimental on histopathological images as shown in Fig. 3.10. In the second experiment the manual options is added to select the best cluster in sort of the intensity value calculated by STD. We observed that the result is improved in true positive rate (TPR) to 0.88 and in the F1-score (F-M) which is basedon the (TPR) and positive prediction value (PPV) reached to 0.93 on UCSB 58 sets also in dice similarity coefficient (DSC) reached to 0.93. Whereas, on CRC the TPR =0.46, F-M = 0.61 this approached named semi-automatic. In the last experimental, the automatic approach is applied by calculated the standard deviation and sorted the result to select one before the maximum one automatically, in this test TPR = 82 and F-M = 0.89 on UCSB 58 sets and TPR =0.45 and F-M 0.52 on CRC 100 sets. in this study we have detected the center of nuclei based on the information of the coordination (x,y) in two histopathological data sets (UCSB 58 sets high resolution) Fig. 3.11, and (CRC 100 sets) the result as shown below in Table 3.1.

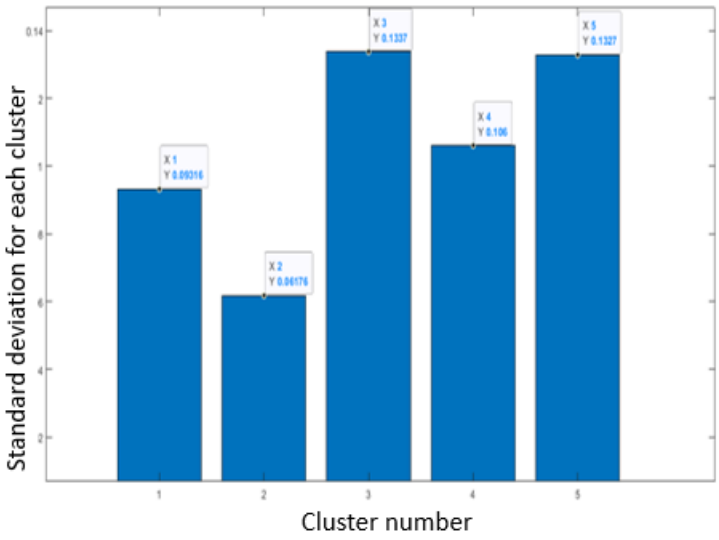

Figure 3.10 Standard deviation results for each cluster illustrated the intensity value for each cluster

Table 3.1 Fuzzy c means results to detect center of nuclei using two different size of histopathological images

Data Set	TPR	PPV	F-M	DSC
UCSB-58 set with FCM semiautomatic	0.881	0.994	0.933	0.933
UCSB-58 set with FCM automatic	0.828	0.994	0.899	0.899
CRC-100 set with FCM semiautomatic	0.466	0.994	0.617	0.617
CRC-100 set with FCM automatic	0.451	0.994	0.528	0.528

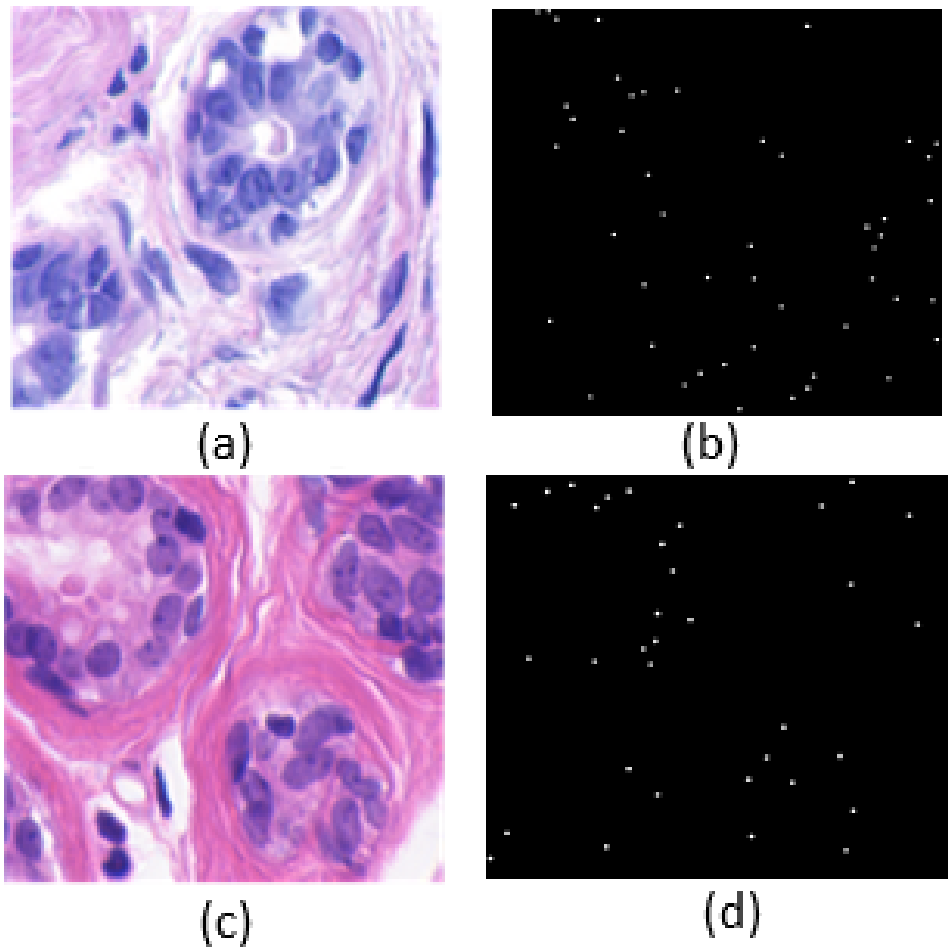

Figure 3.11 (a) Original image, (b) Center image obtained from FCM-automatic (c) Original image obtained from FCM-semiautomatic.

3.4.3 Nuclei center detection via tiny convolutional neural networks (Tiny-CNN)

In recent years, cell structure analysis is represented as a challenge to researchers of pathological images. It is a very important task in this area of computer vision. The main work of this section, an automated efficient algorithm is proposed the cell structure, is described as cell or non- cell based on coordination (x, y) in histopathological images data set information. In this study, two different sizes of histopathological images are used. The first data set obtained from David Rimm Laboratory in Department of Pathology at Yale University of California, Santa Barbara 200×200. However, the second one is obtained from the Department of Computer Science at the University of Warwick 500×500.

The tiny-convolutional neural network (Tiny-CNN) is used, for recognizing the structure of tissues to obtain nuclei in histopathological images and detecting the center of the cell. In the proposed method, the first part introduces typical CNN building blocks and the rectified linear unit (ReLU) functions is applied, where the rule is not a separate component of the convolutional neural networks processes it's one of the supplementary stages of the convolution processes. In this part, it is normally using a gradient-based optimization method or back-propagation algorithm. On another hand, the second part of this work started with learned two basic convolutional neural networks (CNN). The first one is a simple non-linear filter capturing the image structures of nuclei in the related image contain, the second one is a network that recognizes the positive blobs and negative blobs (using a variety of different color white for positive blobs and black for negative blobs) as shown in Fig. 3.12. In the input layer, there is no parameter learning in here, it is used for reading image "x". Whereas convolution layer takes feature map "l" as input for this layer and the bank "K" feature map stands as output, k is a multiple-dimensional filter, the size of filters is "$m \times n$". In our input we have 27 dimensions with filters $3 \times 3 \times 27$. The total weights in such case can be stands as (filter size × filter dimension × input feature maps with a bias for each feature map), it can compute the total number of parameters in here as $(n \times m \times x_l + 1) \times k$).

$$f(x) = f_l(...f_2(f_1)(x; w_1); w_2)....w_L \tag{3.5}$$

In this Eq. 3.5 feed-forward neural network takes function f_l, where x_l represents as input parameter and w_l denoted to weight parameter, in order to produce a new x as output $x_l + 1$. In convolution part data has 2D arrays of pixels size, where each x_i has a real array of pixels $M \times N \times K$, where $M \times N$ denoted as pixel size and K as channels

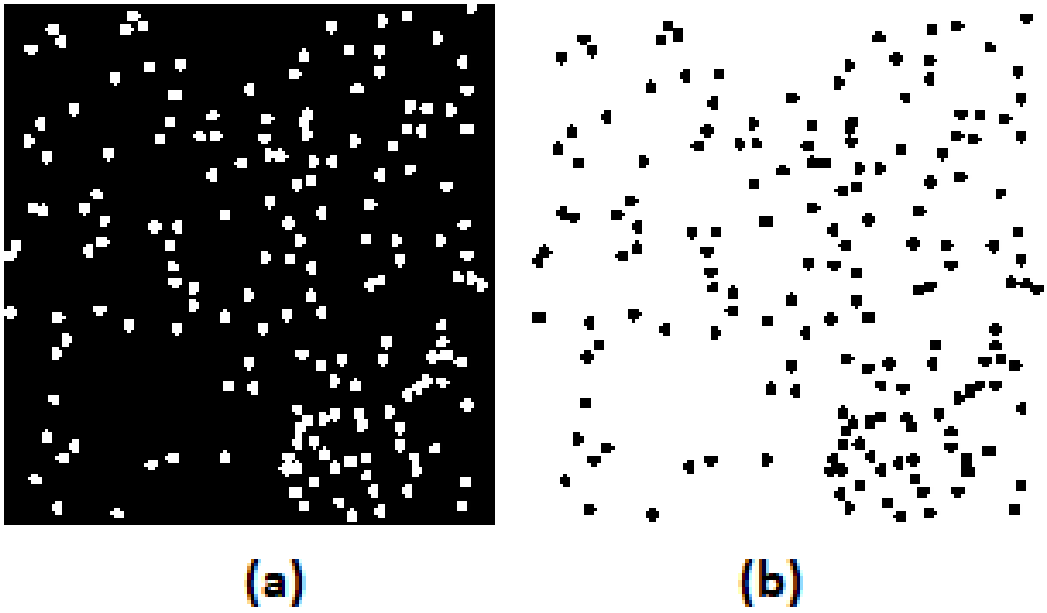

Figure 3.12 (a) Positive blobs, (b) Negative blobs

per pixel. Besides that functions f_l have a convolutional structure to apply the input, feature maps an operator that is local and translation invariant. The convolutional operators can be work as applying a bank of linear filters to each x_l input parameter. The first linear convolution is proposed with filter bank k. This operation can be presented as shown in Eq. 3.6 and Eq. 3.7.

$$x_i \epsilon R^{M \times N \times K}, f : R^{M' \times N' \times K'}, y \epsilon R^{M'' \times N'' \times K''} \tag{3.6}$$

Here, each f functions in convolution part have a bank of linear filter R, when the input data $x_i \epsilon R$ where K is denoted as multiple-dimensional filters such as $(n \times m)$ or $(D \times D'')$.

$$y_{i''j''d''} = b''_d + \sum_{i'=1}^{H'} \sum_{j'=1}^{w'} \sum_{d'=1}^{d'} f_{i'j'd} \times x_{i''+i'-1, j''+j'-1, d', d''}. \tag{3.7}$$

Here, X is represented as array of $H \times W \times D$ where (H,W) are the height and width of the image set, D is the image deepness (number of feature channels). With f is denoted as a single array of dimension $(fW) \times (fH) \times (fD) \times (D \times D')$ and (fH,fW) are the filter height and width, $(D \times D') = k$ is the number of filters in the bank, and (fD) the depth of a filter (the same as the depth of image X). As we can see in the

tiny-CNN learning with the first part, the forward pass in Eq.3.13, it is proposed linear filtering with two terms wight (W is a 27×27) filter and (B) (scalar) bias adds to X_l represent as input array $M \times N$ feature maps. Besides that, Relu function is applied and maxpooling for reducing the number of parameters. The training end-to-end by backpropagation and stochastic gradient descent (SGD) algorithms and the CNN loss function derivative DZDY is applied through the network as we can see in Eq. 3.8.

$$y = w \times x_1 + b \tag{3.8}$$

Here, w stand as weight 27×27, b represent as scalar $x_1 = x$ has a single channel.

$$y = Max\{0, x\} \tag{3.9}$$

Non-linear activation functions in a tiny-CNN it is used, linear filtering with ReLU function input image as shown in Eq. 3.9. Where (W) is a $Q \times Q$ filter along with (B) it's a scalar(bias), X_l is a $M \times N$.

According to pooling layer it is inserted in-between each successive convolution layer, which it is used to progressively decrements the spatial size of the representation to reduce the number of parameters and operations in the network. In this work it can be implemented max and sum pooling. The max pooling operator helps to compute the maximum response of each feature channel in a $H' \times W'$ of each the input image Eq. 3.14 are proposed the maxpooling in tiny-CNN.

$$y_{i''j''d''} = Max_{1 \le i' \le H, 1 \le j' \le W} x_{i''+i'-1, j''+j'-1, d'} \tag{3.10}$$

$$x_3 = maxpool_{\rho} x_2 \tag{3.11}$$

Here, in Eq. 3.11 using the maxpooling operation.

$$Lossfunction = \frac{(res.x3 > 1 \& pos)}{\sum(pos)} - \frac{res.x3 > 0 \& neg}{\sum(neg)} \tag{3.12}$$

Here, in Eq. 3.12 we can see the loss function of convolution layer. Where (Neg) represent as a negative blobs and (Pos) as a positive blobs. all the (TINY-CNN) operation illustrated in Fig. 3.13.

In some cases filter does not perfectly fit with the input image, the padding and stride helps to solve this issue, are works to specify top, bottom, left and right padding such as: $(P_h^-, P_h^+, P_w^-, P_w^+)$ of the input set and subsampling strides (S_h, S_w) of the output array as shown in Eq. 3.13.

$$y_{i''j''d''} = b_d'' + \sum_{i}^{'} = 1^{H'} \sum_{j'=1}^{W'} \sum_{d'=1}^{D'} f_i' j' d \times x_{S_h(i''-1)+i'-P_h^-,(j''-1)+j'-P_w^-,d',d''}. \tag{3.13}$$

In Eq. 3.13, the input array x is implicitly extended with zeros as it is needed.

Output Size Image: In a convolutional neural network, there are three main parameters that helps to modify the behavior of a convolutional layer. These parameters are filter size, stride and zero padding. The size of the output feature map generated depends on the above three important parameters. In this part of work, only the "valid" part of the convolution is used to compute. Where it keeps each implementation of a filter to be fully contained in the input support. The size of the output image in convolutional layer can be computed in Eq. 3.14.

$$H'' = 1 + \left[\frac{H - H' + P_H^- + P_h^+}{S_h} \right] \tag{3.14}$$

In Eq. 3.14 H' represent a bet vertical filter dimension, with symbol S_h stand as a subsampling stride, and P_h^-, P_h^+ denoted to the number of zeros padding implemented to the top and the bottom of the set input image(x). The important thing here to observe that the padded input must be at least as large as the filters: $H, P_h^-, P_h^+ \geq H'$, rather that it lead to error in the convolutional layer.

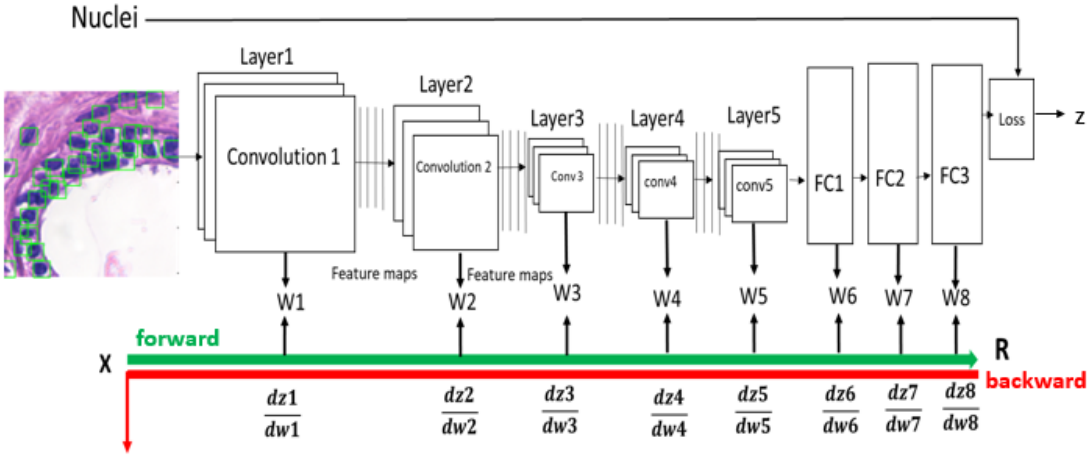

Figure 3.13 Tiny-CNN learning to detect center of nuclei in histopathological image

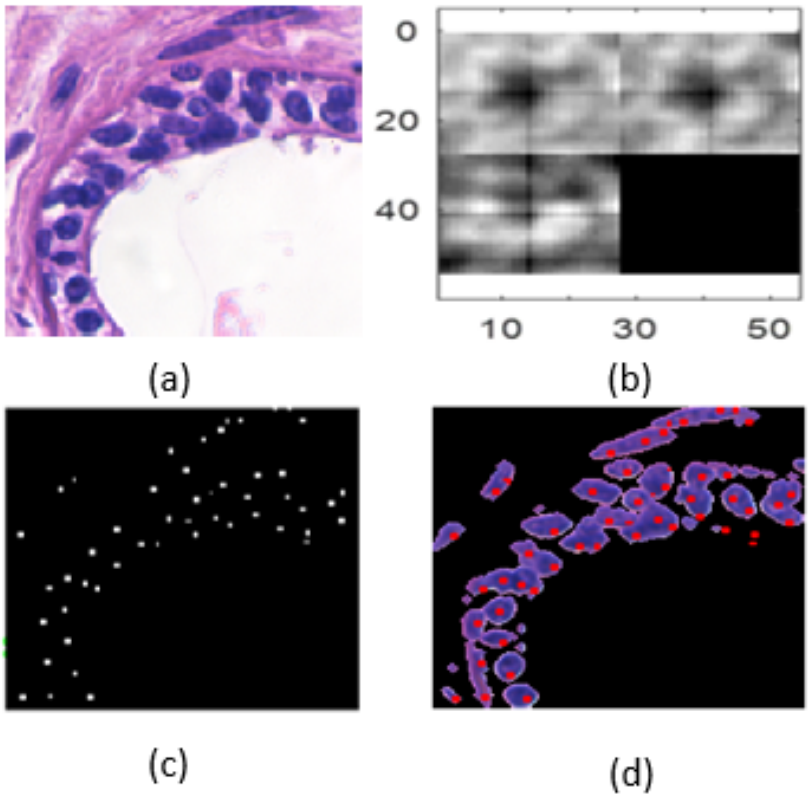

Figure 3.14 (a) Original image UCSB data set, (b) filtered nuclei in tiny-CNN process, (c) center nuclei in tiny-CNN process (d) mask nuclei after tiny-CNN

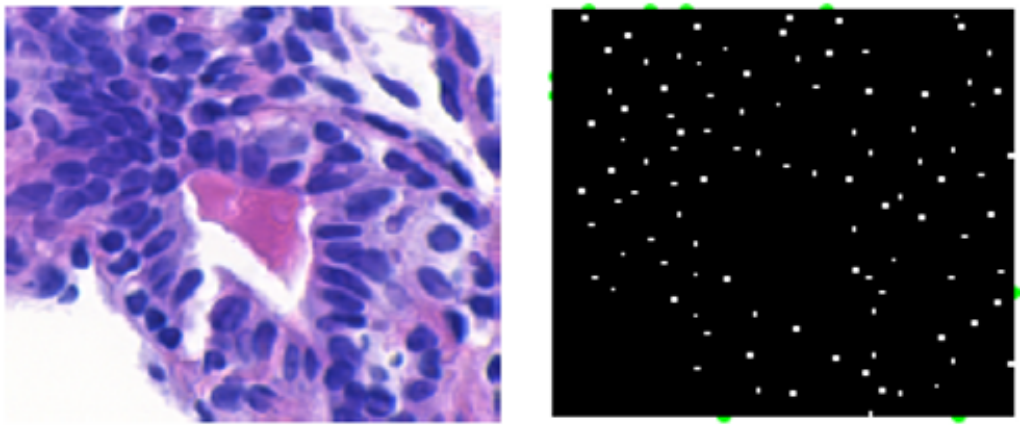

Figure 3.15 (a) Original image UCSB data set, (b) center nuclei after Tiny-CNN process

3.4.4 Detection and evaluation results obtained by tiny-CNN

The objective of this study, is to detect all nuclei in an image by using the coordination (x,y) information in each of histopathological images (UCSB) and (CRC). Evaluation part of detection is measured true positive rate, positive prediction rate, F1 score, and dice similarity coefficient. were used to quantitatively assess the performance of this part. Here, we dene the region of nuclei within the radius of 10 pixels in the CRC data set and 20 pixels in the USCB data set.

Table 3.2 Nuclei Center Detection Results with UCSB-58 and CRC-100 Histopathological Image Data Sets by using Automated Method Tiny-CNN

Data Set	TPR	PPV	F-M	DSC
UCSB-58 set with Tiny-CNN	0.964	0.996	0.979	0.979
CRC-100 set with Tiny-CNN	0.621	0.989	0.769	0.769

3.4.5 Nuclei center detection via combined (FCM) unsupervised method with (CNNs) supervised method.

In this part of the study, unsupervised behavior method such as fuzzy c means along with a convolutional neural network supervised method are used together to detect the center of nuclei in histopathological images, In order to reach more information on cell structures of nuclei, In this case, the output of (Tiny-CNN) has combined with the output of fuzzy c means semi-automatic approaches to detect the center of nuclei as shown in Fig. 3.16. For increasing, the details of cell structure the nuclei output in histopathological images are masked to obtain accurate nuclei results.

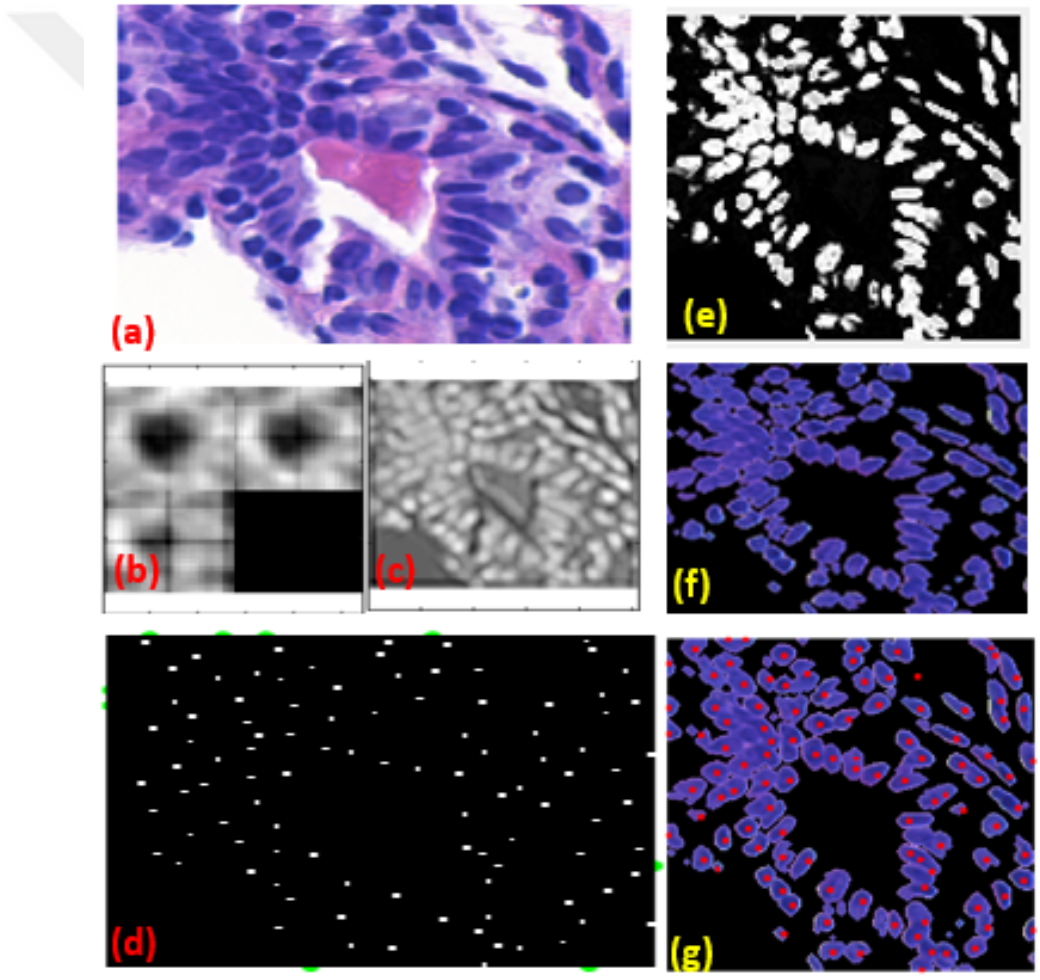

Figure 3.16 (a) Original image from UCSB-58 data set, (b) the result of filtering, (c) Tiny-CNN output image detect of nuclei, (d) final output result of Tiny-CNN detect center of nuclei, (e) FCM semiautomatic result, (f) generated mask from the FCM semiautomatic result combined with original image g) used mask image with Tiny-CNN output the center of the nuclei detection

3.4.6 Evaluated results of nuclei center detection via combined (FCM) unsupervised method with supervised method

For numerical comparison and to illustrate the performance of our model proposed for nuclei center detection by using fuzzy c means clustering method and automated method based on tiny-convolutional neural network. The basic experimental results unit in this study, has used the boundary of cell size to detected the correct nuclei in related image. In the first data set UCSB-58 data set we stand a region information around 20 pixel as circular regions we can see that in (a) Fig. 3.17 Whereas, in the second data set CRC-100 data set, we stand the circular regions within 10 pixels as shown in (b) Fig. 3.17 of each cell in the histopathological image.

A detection can be evaluated of cell center is identified to be a true positive (TP) when it is matched within the ground-truth information, otherwise, it is represent as a false positive (FP). Every true positive is incorporated with the nearest ground-truth cell center. The ground-truth cell centers that are not matched by any detected results are represented as false negatives (FN). The accuracy of nucleus detection is calculated on a per nucleus basis on recording the true positive (TP) (correctly identified nucleus detected), false negative (FN) (incorrectly rejected nucleus), and false positive (FP) (identified no match in our model detection with ground truth information). In Fig. 3.18 the ground-truth results with Tiny-CNN results. In this study the automated method, contributors achieve results as shown in Table 1. Focusing on the F-M measure we have also defined True Positive Rate (TPR) and Positive Prediction Value (PPV). Based on the above definitions, we observe the strongest performance reach to (FM between 0.769 and 0.979) as shown in Table 3.3.

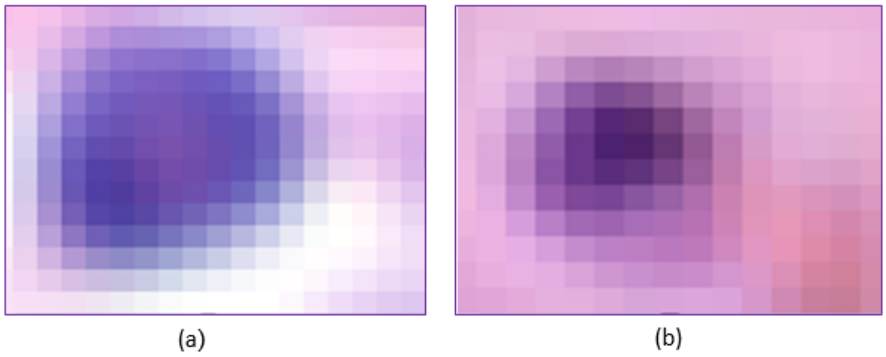

Figure 3.17 (a) Boundary of cell size in UCSB data set to detect the correct nuclei, (b) boundary if cell size in CRC data set to detect the correct nuclei in histopathological images

The sensitivity or true positive rate (TPR) is estimated by formula as in Eq. 3.15:

$$TPR = \frac{TP}{TP + FN} \tag{3.15}$$

F1-score in Eq. 3.17 is represented as a metric of overlap between the nuclei predicted and ground-truth information. The F1-score is associated with true positive rate and precision prediction value in Eq. 3.16.

$$PPV = \frac{TP}{TP + FP} \tag{3.16}$$

$$F1 - score = 2 \times \frac{TPR \times PPV}{TPR + PPV} \tag{3.17}$$

$$DSC = \frac{2TP}{2TP + FP + FN} \tag{3.18}$$

Dice Similarity Coefficient (DSC) in Eq. 3.18 is used as a statistical validation measurement for evaluating the performance of both the predictability of manual segmentation and the overlap accuracy of automated segmentation of histopathological images.

All information about the experimental results about detection of nuclei in histopathological images in this study, are shown in Table. 3.3 each different method in this study performs differently. In this paper, the proposed methods has obtained true positive rate (TPR) of nucleus center detection has reached to be between (0.863 - 0.964) at UCSB-58 data set consisting of 58 images. In addition, in this data set the (F-M or F1-score) has reached to 0.979 in Tiny-CNN and 0.934 in the combined FCM and Tiny-CNN and others FCM approaches are reached between (0.89 - 0.933), whereas,in CRC data set the true positive rate (TPR) has obtained results between (0.547 - 0.621) and (F-M) has reached between (0.528 - 0.769), in this instance, the evaluating of boundary in this study, has a directly effect the true positive rate (TPR) as shown in Table 3.3.

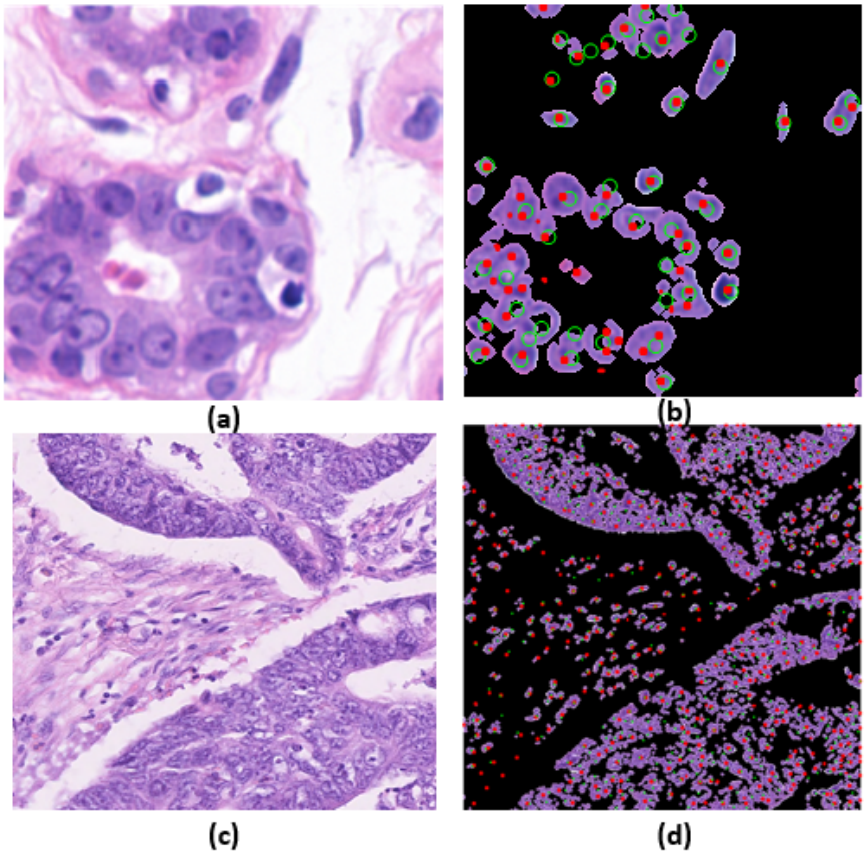

Figure 3.18 a) An example image of UCSB-58 data set and, b) red points represent outputs of nucleus center detection by Tiny-CNN; green circles refer to ground truth information. c) An example image of CRC-100 data set and, d) output of detected nucleus centers Tiny-CNN and ground-truth

Table 3.3 Nuclei detection results with UCSB-58 and CRC-100 histopathological image data sets by using Tiny-CNN and FCM semiautomatic, automatic method, and, combined FCM semiautomatic with Tiny-CNN

Data Set	TPR	PPV	F-M	DSC
UCSB-58 set with Tiny-CNN	0.964	0.996	0.979	0.979
UCSB-58 set with FCM semiautomatic	0.881	0.994	0.933	0.933
UCSB-58 set with FCM automatic	0.828	0.994	0.899	0.899
CRC-100 set with Tiny-CNN	0.621	0.989	0.769	0.769
CRC-100 set with FCM semiautomatic	0.466	0.994	0.617	0.617
CRC-100 set with FCM automatic	0.451	0.994	0.528	0.528
UCSB-58 set with combined FCM and Tiny-CNN	0.863	0.994	0.934	0.934
CRC-100 set with combined FCM and Tiny-CNN	0.547	0.967	0.741	0.741

Table 3.4 Comparative results for nucleus detection with other studies

Method	TPR	PPV	F-M
SSAE [10]	0.644	0.617	0.630
SR-CNN [77]	0.804	0.783	0.793
LIPSyM [78]	0.517	0.725	0.604
CRImage [79]	0.461	0.657	0.542
CP-CNN [80]	0.687	0.697	0.692
Combined FCM and Tiny-CNN	0.547	0.967	0.741

3.5 Discussions

• First experiment

The performance of the UCSB data set, in here we considered the pathologist's notation as ground truth (GT). Pathologists provided that notations on a total of 58-set of study images. For these 58 images, we evaluated the performance of research fellows, the automated method, and FCM method concentrate on the F-M measure (it is incorporated bothTPR and PPV), we observe the strongest performance for the research reached to (FM between 0.97 and 0.93) on UCSB-58 set with size 200×200 as shown in Fig. 3.19.

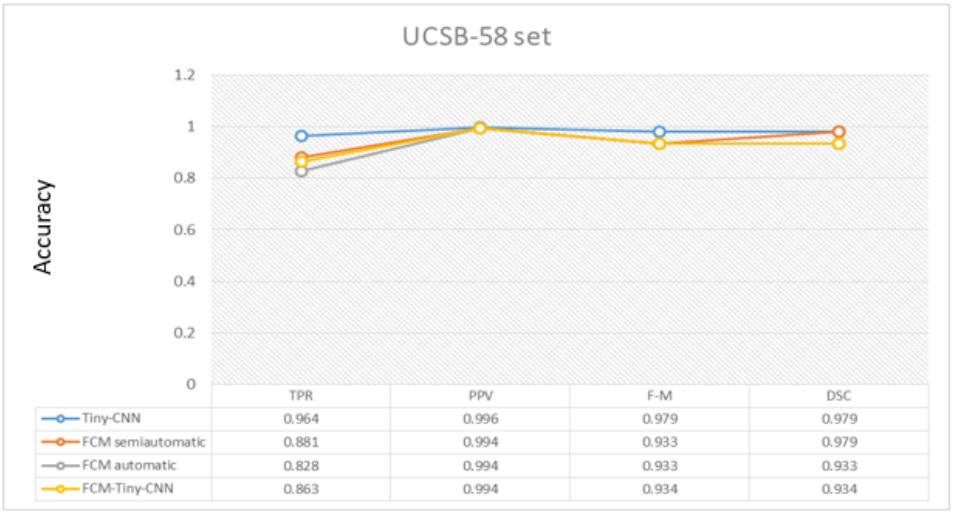

Figure 3.19 Result of all the methods of the first approach on the UCSB data set

• Second experiment

In the second performance, we worth considering the notations from research fellows as GT. The research fellows provided notations for all of 100 images containing 22,444 nuclei centers, denoted as GT nuclei in this experiment. Thus, the data set for this evaluation is significantly larger than that for the initial analysis, which used the pathologist annotation as the GT. In this performance with $F-M$ scores the strongest performance for research reached to (FM between 0.769 and 0.741, as shown in Fig.3.20.



	TPR	PPV	F-M	DSC
Tiny-CNN	0.621	0.989	0.769	0.769
FCM semiautomatic	0.466	0.994	0.617	0.617
FCM automatic	0.451	0.994	0.528	0.528
FCM-Tiny-CNN	0.547	0.967	0.741	0.741

Figure 3.20 Result of all the methods of the first approach on the CRC data set

• Image size

To assess the impact of image size on contributor experiment, we performed an approach in which we extracted images of two different sizes (200×200 and 500×500) from the same $ROIs$. We observed that the image in size (200×200) performed significantly better than the larger image in sizes (500×500). and also the experimental method by using the boundary of cell is directly effected on the TPR as shown in Table 3.3.

4
Classification of Nuclei in Histopathological Images

In this section we aimed two different types of machine learning approaches for automatic nuclei classification in histopathological images on University of Warwick's colon data set with four nuclei types: Epithelial, inflammatory, fibroblast and other. The first step in this approach was based on a pre-trained convolutional neural network-based feature extraction with support vector machine-based classification. In the second step of this approach, local phase quantization (LPQ) is applied along with support vector machine-based classification with data set augmentation. The obtained results achieved high accuracy rates reached to on the classification of nuclei in histopathological images.

4.1 Data Set and Prepossessing in Histopathological Images

In this study, we have used histopathological colon data set as shown in Fig. 4.1, obtained from Tissue Image Analytics (TIA) Lab in University of Warwicks [15]. The data set contains 100 H&E stained histopathological images of colorectal adenocarcinomas. It involves a total of 22444 labeled cell nuclei in all histopathological images and the size of patches in each set is 32×32. Each nucleus in images belongs to one of the four different types of nuclei. These types are labeled as epithelial, inflammatory, fibroblast and others as presented in Fig. 4.2. The label of 'others' represents the nuclei that do not belong to the three different nuclei types such as epithelial, inflammatory and fibroblast. In the data set information, there are 7722 epithelial, 5712 fibroblast, 6971 inflammatory, and 2039 other nuclei types [81].

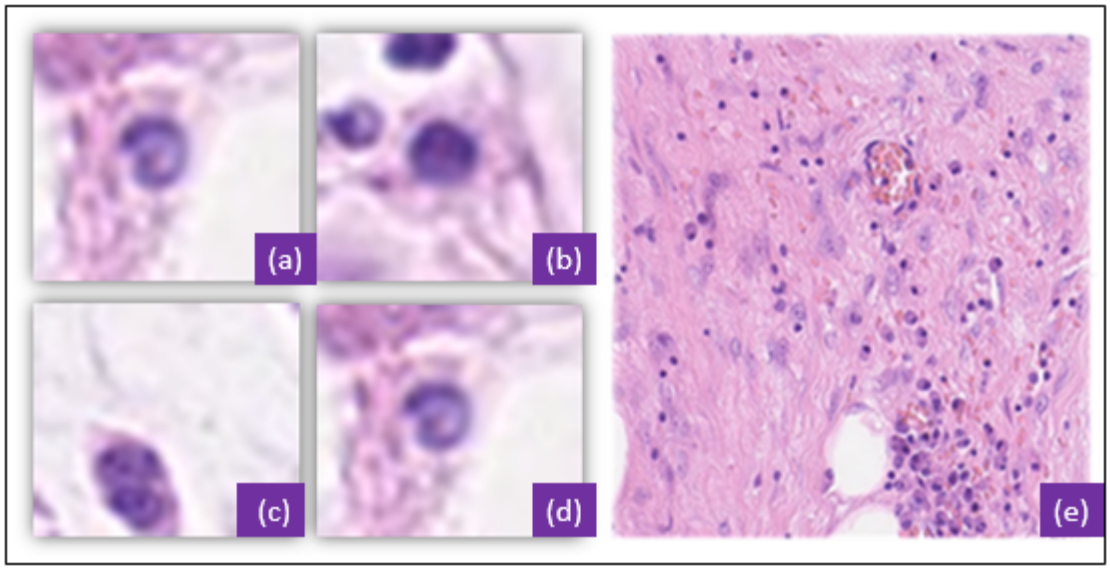

Figure 4.1 (a,b,c,d) four different types of nuclei, (e) the original image of histopathological images

As a pre-processing step, it is a common approach augment the data set for increasing the classification performance of deep learning strategy:

• In order to augmenting the data set patches, patches have been rotated in 0°, 90°, 180°, 270°.

• Besides that, we have applied horizontal flipping, vertical flipping and also diagonal flipping as shown in Fig. 4.3; finally we could augment the number of patches as shown in Table 1. In order to avoid the overfitting data set, input image patches of data set are split into 70% for training and 30% for testing, repeatedly.

Table 4.1 Information Table of Augmented Data Set

Data Set	Patches before augmentation	Patches after augmentation
Epithelial	35 patches	840 patches
Fibroblast	73 patches	923 patches
Inflammatory	83 patches	764 patches
Others	63 patches	1140 patches
Total	254 patches	3667 patches

The data set contains 100 *H*&*E* stained histopathological images of colorectal adenocarcinomas.

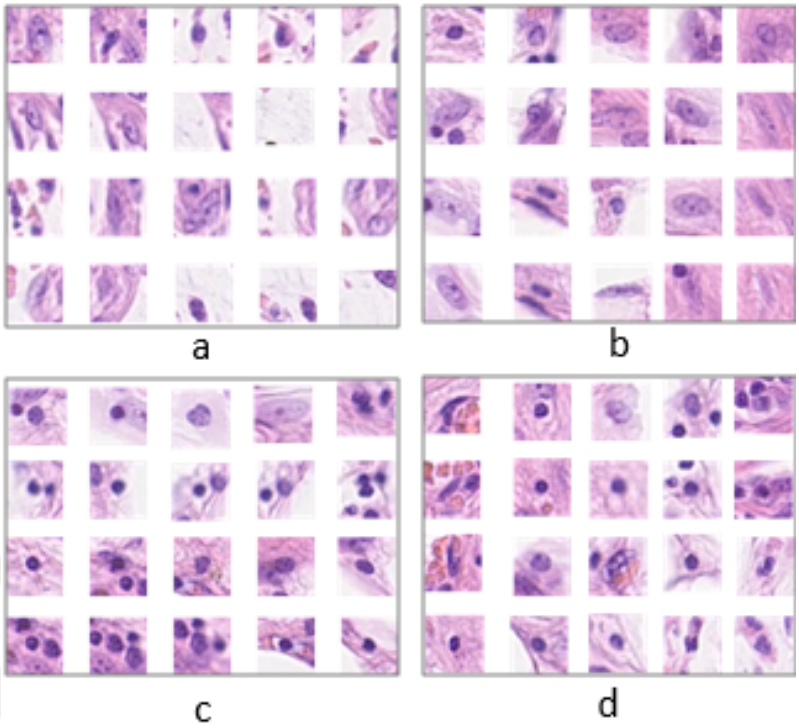

Figure 4.2 Example of data set patches consist of four types of nuclei stand as: (a) epithelial, (b) fibroblast, (d) inflammatory, (c) others.

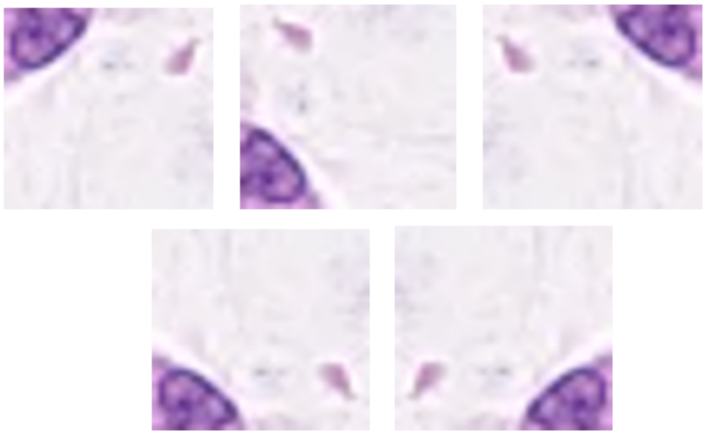

Figure 4.3 Proposed a histopathological patches images after applying augmented methods.

4.2 Local Phase Quantization (LPQ)

The LPQ operator is a texture descriptor robust to image blurring, it is one of the efficient image descriptor in machine learning proposed in 2008 by (Ville Ojansivu and Janne Heikkila). Local phase quantization (LPQ) can be used to extract the features based on sets of three orthogonal levels denoted as (XY,XZ and YZ) [82]. After the combination of these individual levels of histograms together, a single histogram for these levels can be obtained as shown in Fig. 4.4. In order to capture textural details at different aspects, different sizes of the window can be exploited to obtain a multiscale representation of textural content of an image. Furthermore, the histograms of each plane are normalized separately. Finally, each sums up to 1 to yield a coherent representation. The LPQ descriptor can be used the local phase information which is extracted by $2D\ DFT$ or more precisely, commonly LPQ bases on the short term Fourier transform STFT which it is computed over a rectangular $M-by-M$ neighborhood N_x at each pixel position in the related image content ($F(x)$ as it is shown in Eq. 4.1.
.

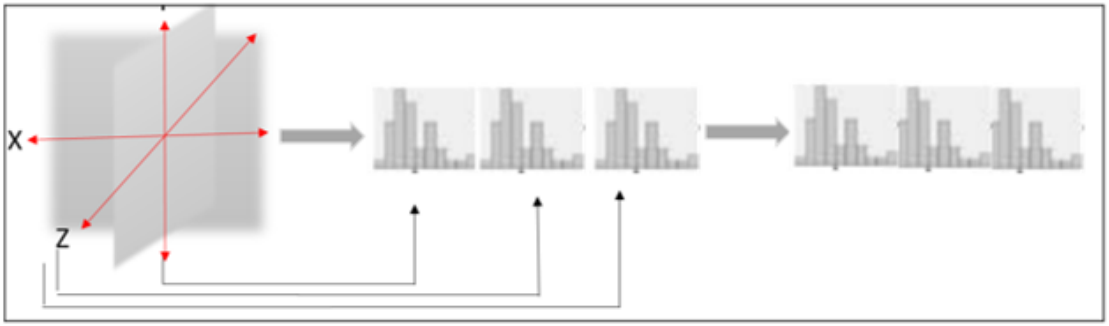

Figure 4.4 selected features by proposed a histogram on three orthogonal levels

$$F(u,x)=\sum_{y\in N_x} f(x-y)e^{-j2\pi u^y}=w_u^T f_x \tag{4.1}$$

Here, w_u is represented as the basis vector of the $2-D\ DFT$ at frequency u with f_x is denoted another vector containing all M^2 image samples from N_x.

In Eq. 4.1 it can be seen, a simple way of implementing the STFT is to use $2-D$ convolutions $f(x-y)e^{-j2\pi u^y}$ for all u. In LPQ only four complex coefficients are considered, corresponding to 2-D frequencies. $u_1=[a,0]^T, u_2=[0,a]^T, u_3=[a,a]^T, u_4=[a,-a]$ a represent to scale of frequency.

$$F_x^c=[F(u_1,x),F(u_2,x),F(u_3,x),F(u_4,x)], and F_x=[Re(F_x^c),Im(F_x^c)^T] \tag{4.2}$$

In Eq 4.3 $Re(F_x^c)^T and Im(F_x^c)^T$ stand as real and imaginary parts of a complex number, respectively. The corresponding 8-by-M2 transformation matrix is

$$W = [Rew_u1, w_u2, w_u3, w_u4]^T \tag{4.3}$$

That led to

$$F_x = Wf_x \tag{4.4}$$

In this case, blur insensitive texture classification is used local phase quantization. The phase information in the Fourier coefficients is recorded by examining the signs of the real and imaginary parts as shown in Eq. 4.2 of each component in F_x in Eq. 4.4. This is done by using a simple scalar quantiser.

$$q_j = \begin{cases} 1, & \text{if } g_j \geq 0 \\ 0, & \text{otherwise} \end{cases} \tag{4.5}$$

In Eq. 4.5 $q_j(x)$ is the jth component of the vector $F_x = [ReF_x, ImF_x]$. Eight bit binary is obtained as a coefficients $q_j(x)$ are represented as integers using binary coding:

$$fLPQ(x) = \sum_{j=1}^{8} {q_j}^{2^{j-1}} \tag{4.6}$$

The result here in LPQ features, a histogram of these values from all positions is consisted resulting in a 256-dimensional feature vector to obtained the important information of the object in a given image. In this study, LPQ features have used and applied on the augmented data set in histopathological images as it shown in Table 4.1 to classify multi types of nuclei based on support vector machine method and predicted the result. The extended mathematical foundations of LPQ method can be found in [83].

4.3 Nuclei Classification in Histopathological Images via Local Phase Quantization and Convolutional neural network

4.3.1 Nuclei classification in histopathological images via local phase quantization and support vector machine

In our experiments, the scale down process has applied in 32 × 32 input images, before using LPQ algorithm for feature extraction in this stage, a SIFT descriptor is

calculated for each orthogonal as a histogram of orientation in eight directions and orientation are calculated in a region around the related spatial localization (right) a 16 × 16 neighborhood around the related spatial localization is divided to 4 × 4 subregions. In each subregion, the gradient vectors are accumulated into 8-bins orientation histograms. Then 256 features are extracted from the related spatial localization as we can see in 4.6.

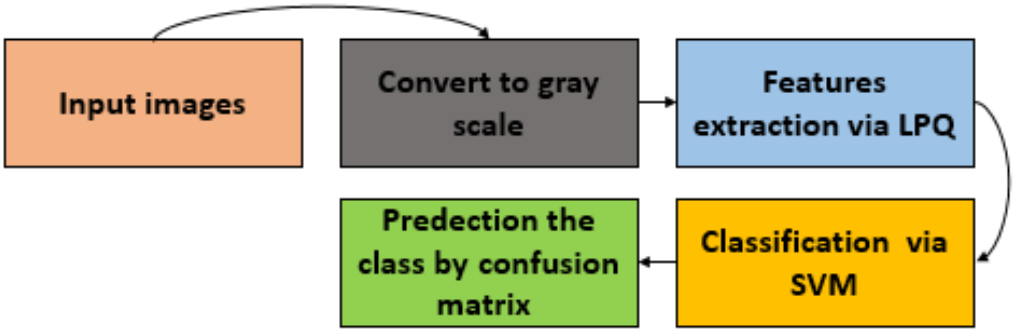

Figure 4.5 Flowchart proposed LPQ-SVM methodology

Classification, in this part as we can see in Fig.4.5 the support vector machine classification with LPQ features extracted from histopathological images Fig. 4.6. Where the support vector machine (SVM) is a supervised method proposed by [84] to find the optimal hyperplane and separate the training parameters in two binary classifications, by maximizing the norm between the hyperplane and the two classes [85]. The input training vector $x_n \in R^d$, n= 1,...,l,$(w, x) = w.x + b$ based feature of training vectors. The SVM method works to solve the solution of optimization problem to learn the parameters of (w) into classes as shown below:

$$min\frac{1}{\rho}w^T w + C\sum_{n=1}^{\rho}(max(0, 1 - \acute{y}_n(w^T x_n + b) \tag{4.7}$$

In equation. 4.7 $w^T w$ is the weight vector $\in R^d$, C stand as the regularization value, $w^T x_n + b$ mapping function to predict features. In this part of classification our model selecting all the features at the first test and we got an accuracy of around 53.9% which is not pretty good for a predictive model and after doing some feature for example; two classes instead of four classes selection without doing any logical changes in my model code my accuracy jumped to 85%-95% by using confusion matrix. Along with this study, the confusion matrices which are used to obtain a summary of prediction results on a classification problem, it used to help understanding the detailed accuracy of selected classifiers in each class of the data set. In addition, the plots of the confusion matrices can identify the region where the classifier performed poorly and give an

evaluation of this performance. The rows show the true (actual) classes and the columns show the predicted classes, whereas, the diagonal cells show where the actual classess and predicted classes match together. This part of this study, is extracted features for multi types of nuclei in histopathological images.

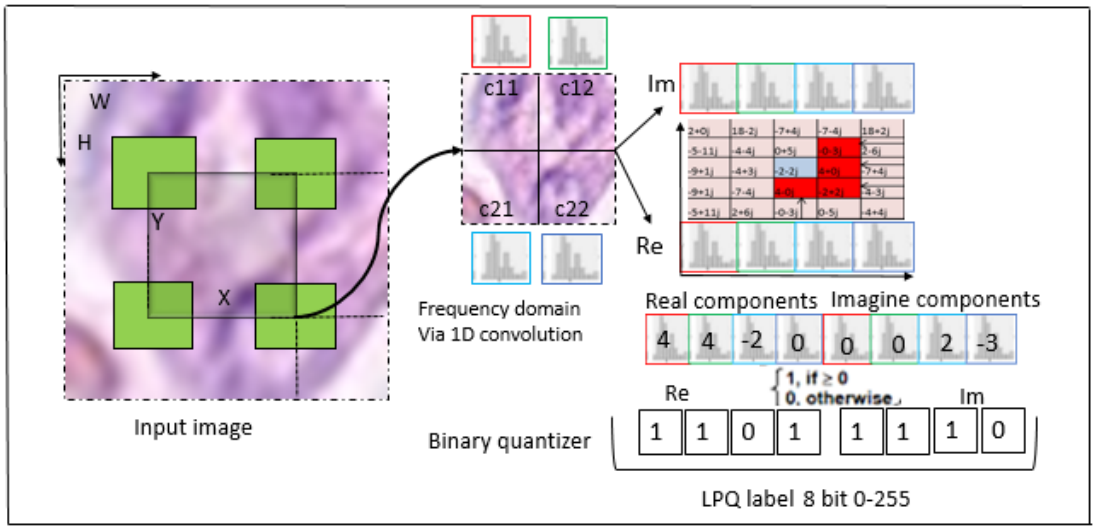

Figure 4.6 Spatial localization of the selected features by proposed a histogram on three orthogonal levels

4.3.2 Nuclei classification via convolutional neural network and support vector machine

In feature extraction step via CNN models, we need to train the CNN network with the last dense layer Fig. 4.7. The purpose of training the network is to identify the correct weights for the network by multiple forward and backward iterations. In this study, training and testing image sets of the colon data set were obtained from the Tissue Image Analytics (TIA) Lab at University of Warwick. Image data set is split into 70% for the training data and the remaining 30% for the testing data. The neural network structure consists of two convolutional layers with 32 filters in each layer. Batch normalization is applied after each convolutional layer. Afterwards, rectified linear units (ReLu) are used as the activation function for the convolutional layer. In the output of each convolutional layer, batch normalizing has been applied to avoid the stuck in neuron saturation of later layers in the network as well. As similar to [86], pre-trained models are exploited to extract features: the first one is Residual Network 50 (ResNet50), and the second one is Residual Network 101 (ResNet101) for CNN based feature extraction. The next part of the network consists of fully connected layer with the final output layer consists of four neurons where each class has one neuron. Commonly used softmax layer for multiclass classification was changed with

50 support vector machines for calculating prediction probability for each class. The network is trained with stochastic gradient descent (SGD) algorithm with 32 filters of histopathological images. In our study, the classification four different classes of nuclei patches of the histopathological colon data set. Multiclass SVM classifier is used to classify CNN based features. In training phase, a fast Stochastic Gradient Descent (SGD) solver is used by setting the fitcecoc function's 'Learners' parameter to 'linear'. In this way training stage can be accelerated when working with high-dimensional CNN based feature vectors. The training of multiclass support vector machine classifier also uses a fast linear solver with radial basis kernel function. In the feature extraction phases of training and testing stages, CNN architectures of ResNet50 and ResNet101 are used to extract features on histopathological image to classify four classes as shown in Fig. 4.12. The results reached up to 85% overall accuracy with a duration processing of 1.45 seconds. We have also tested the inflammatory and others; it took 16.61 seconds with results reaching up to 95%. The class match reached between 85% and 95% for this approach based on confusion matrix has been shown as in Fig. 4.11. In addition, we have implemented the same scenario along with using four nuclei classes with augmented data set. We have observed that the results showed a tendency to decrease as shown in the confusion matrices which are plotted in Fig. 4.9 and Fig. 4.10 with process duration of 1.72 seconds. Comparing the achieved results, we have observed that the classification for two classes with original data set LPQ-SVM model was better than the CNN-SVM with two classes of original images data set. However, the convolutional neural network using support vector machine with augmented data set which has obtained improved results.

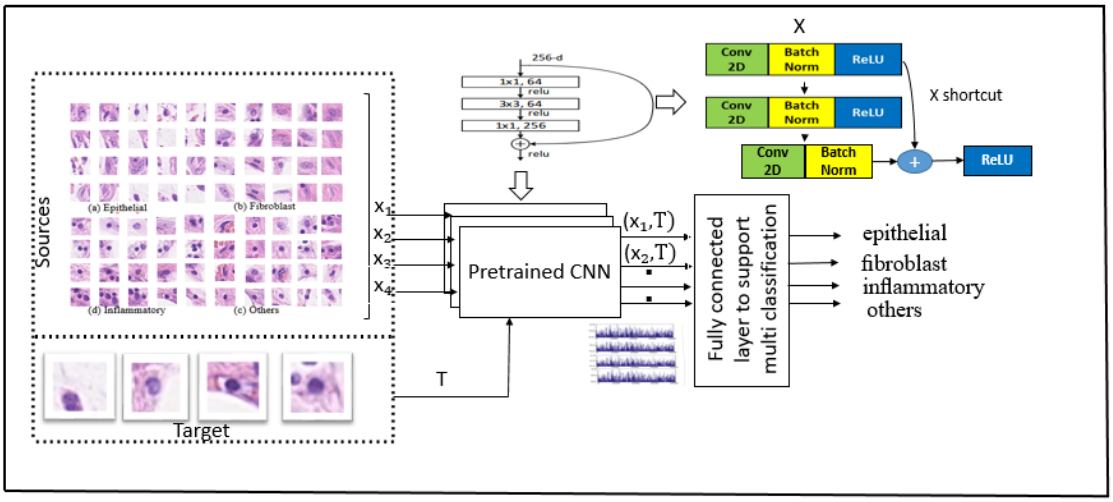

Figure 4.7 ResNet convolutional neural network based model to classify four types of cells in histopathological images along with augmented data set.

4.3.3 Evaluated the performance results of nuclei classification

In the first step pf the proposed study, we have used the original data set with ResNet50 model for feature extraction. After CNN based feature extraction, classification result by support vector machine results in this test data set reached up to 85% and duration of this process was 35.57 seconds. In addition, we have tested another feature extraction step using ResNet101 model. In this case, the accuracy of CNN-SVM based system has reached up to 75% and the duration of this process was 37.51 seconds in epithelial and other classes. In inflammatory and fibroblast classes, the result has reached up to 82.3% with the duration of 327.37 seconds using net ResNet101 as shown in Fig. 4.8. In the second test, we applied the data set augmentation processes. The results reached between 80.1 and 94.8. The results of each experiment by using confusion matrix are proposed in Table 4.2 and Table 4.3.

Table 4.2 Results of Confusion Matrix with Original Data Set Using CNN-SVM

Classes	True prediction (ResNet50)	Time	True prediction (ResNet101)	Time
Epithelial	100		90.0	
Others	70.0	35.57 Sec	60.0	37.51 Sec
Class match	85.0		75.0	
Inflammatory	54.7		77.4	
Fibroblast	100	191.6 Sec	87.2	327.37 Sec
Class match	58.6		82.3	

Along with this study, the confusion matrices are used to help understanding the detailed accuracy of selected classifiers in each class of the data set. In addition, the plots of the confusion matrices can identify the region where the classifier performed poorly and give an evaluation of this performance. The rows show the true (actual) classes and the columns show the predicted classes, whereas, the diagonal cells show where the actual classes and predicted classes match together. If these cells have red background, the classifier has performed well and classified observations of this true class correctly.

Table 4.3 Results of Confusion Matrices with Augmented Data Set Using CNN-SVM

Classes	True prediction (ResNet50)	Time	True prediction (ResNet101)	Time
Epithelial	90.5		90.5	
Others	99.2	368.2 Sec	99.2	403.5 Sec
Class match	94.8		94.8	
Inflammatory	95.6		86.1	
Fibroblast	64.5	571.5 Sec	84.3	1015 Sec
Class match	80.1		80.1	

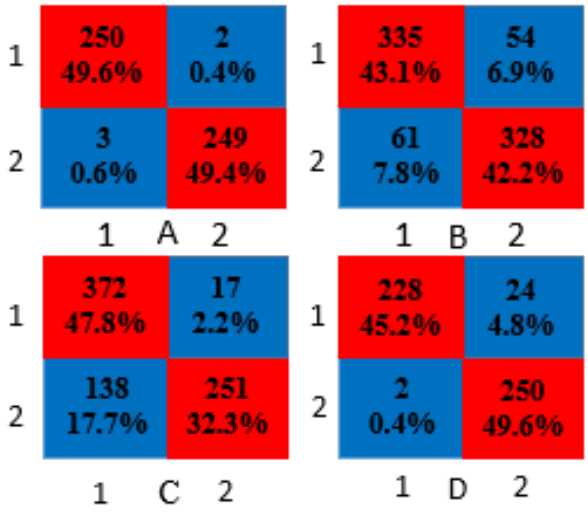

Figure 4.8 Confusion matrices: (A) Confusion matrices of CNN models applied to the augmented data set with ResNet101 for CNN based feature extraction to classify epithelial and other classes, (B) Confusion matrices ResNet101 for CNN based feature extraction to classify inflammatory and fibroblast classes, (C) Confusion matrix using ResNet50 for classify inflammatory and fibroblast, (D) Confusion matrices for classify epithelial and other based on augmented data set.

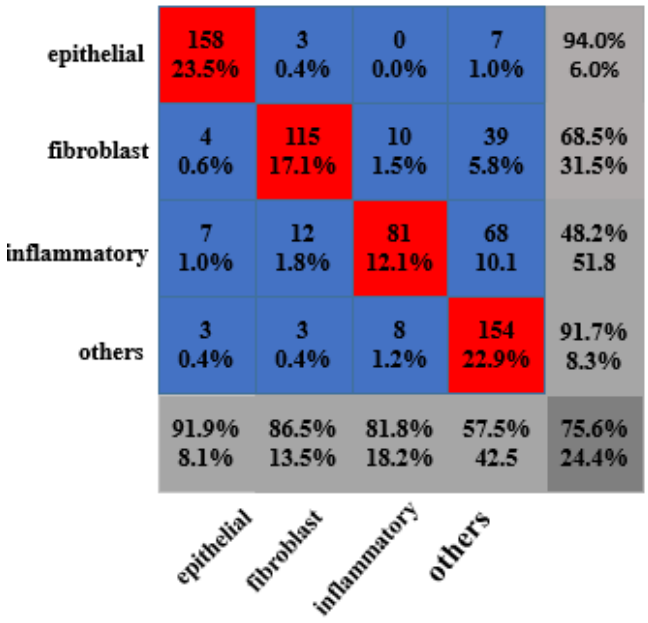

Figure 4.9 Confusion matrices for CNN-SVM based model to classify four types of cells in histopathological images along with augmented data set.

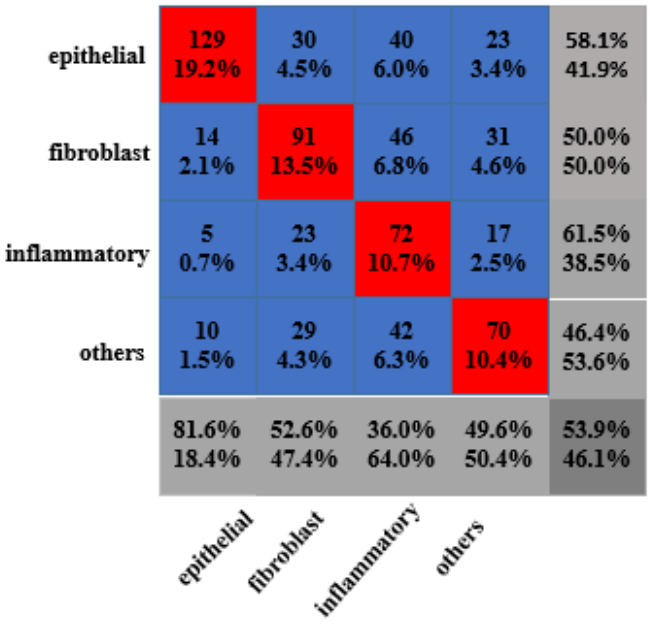

Figure 4.10 Confusion matrices for LPQ-SVM based model to classify four types of cells in histopathological images along with augmented data set.

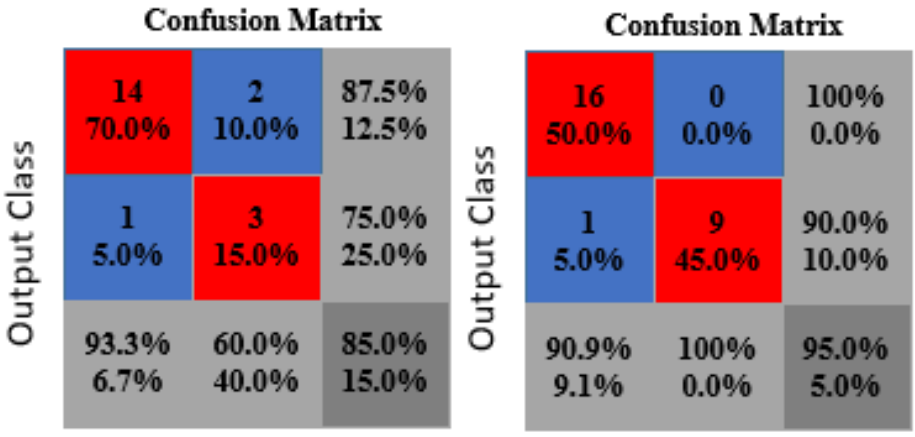

Figure 4.11 Confusion matrices for LPQ-SVM based model for two classes (a) epithelial and fibroblast (b) inflammatory and others with original data set.

4.3.4 Summary of nuclei classification in histopathological images

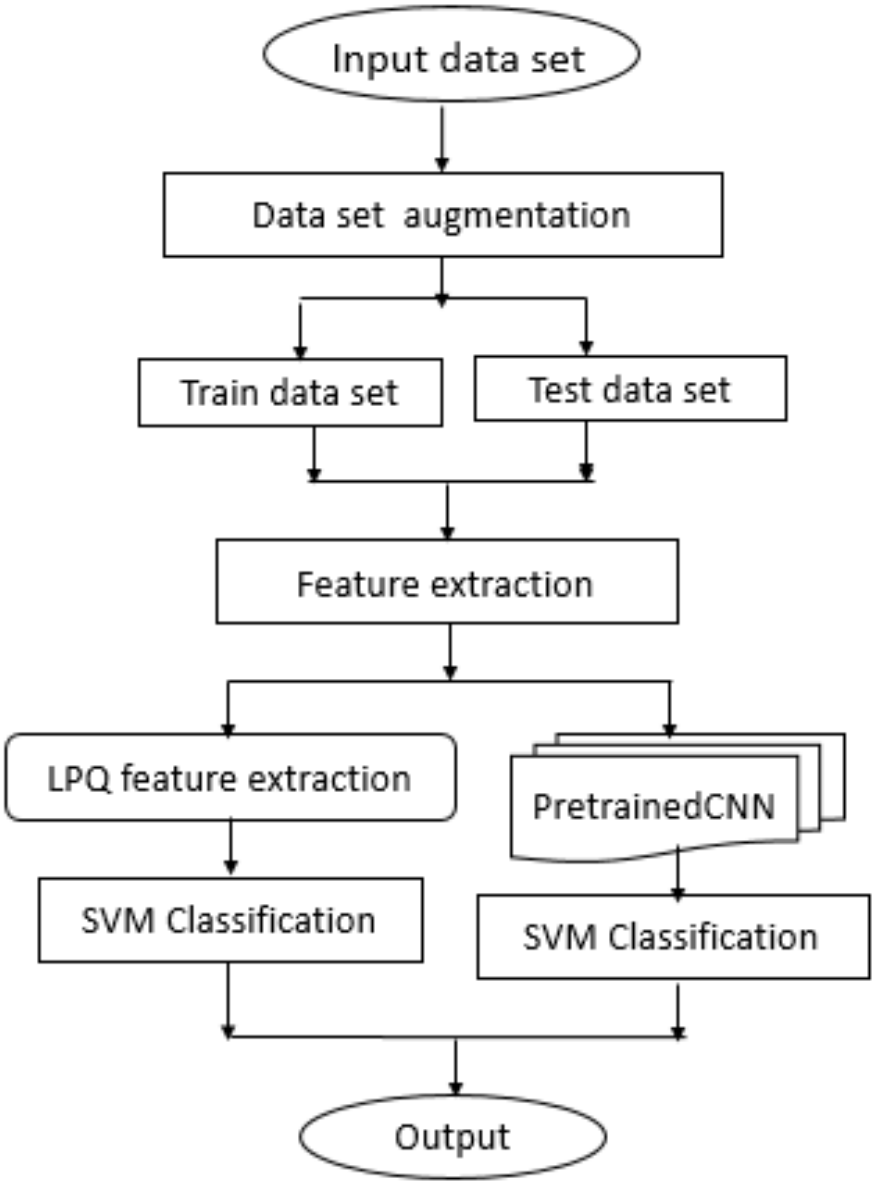

Figure 4.12 Flowchart of the proposed framework of the second part

In this approach, pretrend convolutional neural network and Local phase quantization are used for extracting features in histopathological images and classified it into four types (i.e. epithelial Fibroblast, inflammatory and others). These methods are proposed in Fig. 4.12.

5
Result and Discussion

5.1 Result and Discussion

In this thesis, we studied nuclei center detection and classification methods in histopathological images.

Nuclei center detection and nuclei classification system is designed for solving cluttering problem in pathological images diagnosis. In this study, we evaluated and compared fuzzy c-means (FCM) clustering algorithm with tiny convolutional neural network to detect center of nuclei in histopathological images. To further explore of nuclei in data set images, we combined and experimented two approaches (Tiny-CNN and FCM semi-automatic). High results performance in (F-M) reach to (between 0.899 - 0.979); they are observed in the first data University of California Santa Barbara's UCSB-58 set. However, we also observed in the second, data set University of Warwick's CRC-100 set, the highest results performance in (F-M) between (0.741 - 0.769). In our models, a basis for the qualitative form with similarity between models prediction and ground truth information to detect nuclei in histopathological images are provided. The correct nuclei is detected, according to ground-truth information, it has shown that the prediction of Tiny-CNN method with ground-truth information on the UCSB-58 and CRC-100 data sets. For nuclei classification in histopathological images, in this work, we tested the performance of convolutional neural networks of support vector machine to classify four types of nuclei (epithelial, inflammatory, fibroblast and other) in histopathological data set from University of Warwick. The design of CNNs topology is based on net (ResNet50) and also we tested the performance of net (ResNet101) with binary and multi-class support vector machine (SVM) classification using the original data set of histopathological images and also data set augmented. In the first test we have used the original data set (ResNet50) for feature extraction, in this test the duration was 35.57 seconds with the first two classes which are (epithelial and other), and in this case the class matches reach up to 85%. Whereas, the other classes (inflammatory and fibroblast) the class match reaches up to 58.6% the duration here was 191.6 seconds. Moreover, we tested

the performance of the ResNet101 for the first classes which are (epithelial and other) the class match reaches up to 75% with duration of 37.51 seconds. Whereas, the other ones (inflammatory and fibroblast) the class matches reach up to 82.3% with 327.37% seconds of process duration. On the other hand, we used the augmented data set, we observed that the performance in the first classes reach up to 94% in the class match with process duration of 368.2 seconds it reaches up to 80% in the second classes with duration of 571.5 seconds using ResNet50 model. Whereas, with data set augmented and ResNet101 model the first class reaches up to 94% with process duration 403.5 seconds, and the second class reaches up to 80.1% with duration 1015 seconds. Besides, we applied the augmented data with four classes together to test the performance in the same two models (ResNet50 with SVM and ResNet101 with SVM) we observed the class match with augmented data reaches up to 75% in ResNet50 with SVM and 80% in ResNet101 with SVM. In the classification part we have also used the local phase quantization (LPQ) on histopathological images with support vector machine (SVM) classification. In our proposed method, we observed that the match class works better in case of using convolutional neural network of support vector machines, where the highest class matches classification performance in the classification part is reached to 94.8 %s and 95%.

5.2 Future Works

For the future works of this study, Tiny-CNN can be proposed for the same scenario which we proposed to detect the center of nuclei in histopathological images with comparing the performance of this work with other convolutional neural networks (CNN) established methods, to detect nuclei in histopathological images.

For classification parts in this study, combining the local phase quantization (LPQ) with other feature extraction methods can be a good suggestion for future work. And, comparing the performance of classification between support vector machine (SVM) and conventional machine learning algorithms.

References

[1] M. Veta, P. J. Van Diest, R. Kornegoor, A. Huisman, M. A. Viergever, and J. P. Pluim, "Automatic nuclei segmentation in H&E stained breast cancer histopathology images," *PloS One*, vol. 8, no. 7, e70221, 2013.

[2] A. S. Moita, F. Jacinto, and A. L. N. Moreira, "Design, test and fabrication of a droplet based microfluidic device for clinical diagnostics," in *Proceedings of the 11th Int. Joint Conference on Biomedical Engineering Systems and Technologies-vol. 1: BIODEVICES, BIOSTEC'18*, INSTICC, SciTePress, 2018, pp. 88–95.

[3] A. Albayrak and G. Bilgin, "Mitosis detection using convolutional neural network based features," in *IEEE 17th Int. Symposium on Computational Intelligence and Informatics, CINTI'16*, IEEE, 2016, pp. 335–340.

[4] Y. Al-Kofahi, W. Lassoued, W. Lee, and B. Roysam, "Improved automatic detection and segmentation of cell nuclei in histopathology images," *IEEE Trans. on Biomedical Engineering*, vol. 57, no. 4, pp. 841–852, 2010.

[5] H. Xu, C. Lu, R. Berendt, N. Jha, and M. Mandal, "Automatic nuclei detection based on generalized laplacian of gaussian filters," *IEEE Journal of Biomedical and Health Informatics*, vol. 21, no. 3, pp. 826–837, 2017.

[6] H. Kong, H. C. Akakin, and S. E. Sarma, "A generalized laplacian of gaussian filter for blob detection and its applications," *IEEE Transactions on Cybernetics*, vol. 43, no. 6, pp. 1719–1733, 2013.

[7] J. John, M. S. Nair, P. A. Kumar, and M. Wilscy, "A novel approach for detection and delineation of cell nuclei using feature similarity index measure," *Biocybernetics and Biomedical Engineering*, vol. 36, no. 1, pp. 76–88, 2016.

[8] T. C. Glenn, A. Zare, and P. D. Gader, "Bayesian fuzzy clustering," *IEEE Transactions on Fuzzy Systems*, vol. 23, no. 5, pp. 1545–1561, 2015.

[9] P. Kainz, M. Urschler, S. Schulter, P. Wohlhart, and V. Lepetit, "You should use regression to detect cells," in *International Conference on Medical Image Computing and Computer-Assisted Intervention*, Springer, 2015, pp. 276–283.

[10] J. Xu, L. Xiang, Q. Liu, H. Gilmore, J. Wu, J. Tang, and A. Madabhushi, "Stacked sparse autoencoder (SSAE) for nuclei detection on breast cancer histopathology images," *IEEE Transactions on Medical Imaging*, vol. 35, no. 1, pp. 119–130, 2016.

[11] E. F. Braz and R. Lotufo, "Nuclei detection using deep learning," *Simpósio Brasileiro de e Processamento de Sinais*, pp. 1059–1063, 2017.

[12] J. P. Vink, M. Van Leeuwen, C. Van Deurzen, and G. De Haan, "Efficient nucleus detector in histopathology images," *Journal of Microscopy*, vol. 249, no. 2, pp. 124–135, 2013.

[13] M. Khoshdeli, R. Cong, and B. Parvin, "Detection of nuclei in H&E stained sections using convolutional neural networks," in *IEEE EMBS Int. Conf. on Biomedical & Health Informatics, BHI'17*, 2017, pp. 105–108.

[14] S. Sornapudi, R. J. Stanley, W. V. Stoecker, H. Almubarak, R. Long, S. Antani, G. Thoma, R. Zuna, and S. R. Frazier, "Deep learning nuclei detection in digitized histology images by superpixels," *Journal of Pathology Informatics*, vol. 9, 2018.

[15] K. Sirinukunwattana, S. E. A. Raza, Y.-W. Tsang, D. R. Snead, I. A. Cree, and N. M. Rajpoot, "Locality sensitive deep learning for detection and classification of nuclei in routine colon cancer histology images," *IEEE Trans. on Medical Imaging*, vol. 35, no. 5, pp. 1196–1206, 2016.

[16] A. Albayrak and G. Bilgin, "Automatic cell segmentation in histopathological images via two-staged superpixel-based algorithms," *Medical & Biological Engineering & Computing*, pp. 1–13, 2018.

[17] Y. Goldberg, "A primer on neural network models for natural language processing," *Journal of Artificial Intelligence Research*, vol. 57, pp. 345–420, 2016.

[18] K. Doi, "Computer-aided diagnosis in medical imaging: Historical review, current status and future potential," *Computerized Medical Imaging and Graphics*, vol. 31, no. 4-5, pp. 198–211, 2007.

[19] M. Veta, J. P. Pluim, P. J. Van Diest, and M. A. Viergever, "Breast cancer histopathology image analysis: A review," *IEEE Transactions on Biomedical Engineering*, vol. 61, no. 5, pp. 1400–1411, 2014.

[20] H. Irshad, A. Veillard, L. Roux, and D. Racoceanu, "Methods for nuclei detection, segmentation, and classification in digital histopathology: A review—current status and future potential," *IEEE Reviews in Biomedical Engineering*, vol. 7, pp. 97–114, 2014.

[21] C.-C. Chang and C.-J. Lin, "Libsvm: A library for support vector machines," *ACM Transactions on Intelligent Systems and Technology*, vol. 2, no. 3, p. 27, 2011.

[22] T. Plötz and S. Roth, "Neural nearest neighbors networks," in *Advances in Neural Information Processing Systems*, 2018, pp. 1095–1106.

[23] J. M. Patel and N. C. Gamit, "A review on feature extraction techniques in content based image retrieval," in *Int. Conf. on Wireless Communications, Signal Processing and Networking, WISPNET'16*, IEEE, 2016, pp. 2259–2263.

[24] N. Hatipoglu and G. Bilgin, "Classification of histopathological images using convolutional neural network," in *IEEE 4th Int. Conf. on Image Process. Theory, Tools and App., IPTA'14*, IEEE, 2014, pp. 1–6.

[25] D. Bardou, K. Zhang, and S. M. Ahmad, "Classification of breast cancer based on histology images using convolutional neural networks," *IEEE Access*, vol. 6, pp. 24 680–24 693, 2018.

[26] P. Stone and M. Veloso, "Multiagent systems: A survey from a machine learning perspective," *Autonomous Robots*, vol. 8, no. 3, pp. 345–383, 2000.

[27] T. Mitchell, B. Buchanan, G. DeJong, T. Dietterich, P. Rosenbloom, and A. Waibel, "Machine learning," *Annual review of computer science*, vol. 4, no. 1, pp. 417–433, 1990.

[28] E. Alpaydin, *Machine learning: the new AI*. MIT press, 2016.

[29] Y. Zhang, D. Song, L. M. Lanni, and K. D. Shimizu, "Importance of functional monomer dimerization in the molecular imprinting process," *Macromolecules*, vol. 43, no. 15, pp. 6284–6294, 2010.

[30] X. J. Zhu, "Semi-supervised learning literature survey," University of Wisconsin-Madison Department of Computer Sciences, Tech. Rep., 2005.

[31] V. Mnih, K. Kavukcuoglu, D. Silver, A. Graves, I. Antonoglou, D. Wierstra, and M. Riedmiller, "Playing atari with deep reinforcement learning," *arXiv preprint arXiv:1312.5602*, 2013.

[32] W. S. McCulloch and W. Pitts, "A logical calculus of the ideas immanent in nervous activity," *The bulletin of mathematical biophysics*, vol. 5, no. 4, pp. 115–133, 1943.

[33] B. Widrow and M. E. Hoff, "Adaptive switching circuits," STANFORD UNIV CA STANFORD ELECTRONICS LABS, Tech. Rep., 1960.

[34] J. Sandler and B. Rosenblatt, "The concept of the representational world," *The psychoanalytic study of the child*, vol. 17, no. 1, pp. 128–145, 1962.

[35] R. H. Hahnloser, R. Sarpeshkar, M. A. Mahowald, R. J. Douglas, and H. S. Seung, "Digital selection and analogue amplification coexist in a cortex-inspired silicon circuit," *Nature*, vol. 405, no. 6789, p. 947, 2000.

[36] B. Grote, T. Zense, and B. Hitzmann, "2d-fluorescence and multivariate data analysis for monitoring of sourdough fermentation process," *Food Control*, vol. 38, pp. 8–18, 2014.

[37] F. Rosenblatt, "The perceptron: A probabilistic model for information storage and organization in the brain.," *Psychological review*, vol. 65, no. 6, p. 386, 1958.

[38] J. Orbach, "Principles of neurodynamics. perceptrons and the theory of brain mechanisms.," *Archives of General Psychiatry*, vol. 7, no. 3, pp. 218–219, 1962.

[39] A. G. Ivakhnenko and V. G. Lapa, *Cybernetic predicting devices*. CCM Information Corporation, 1965.

[40] P. Werbos, "Experimental implications of the reinterpretation of quantum mechanics," *Il Nuovo Cimento B (1971-1996)*, vol. 29, no. 1, pp. 169–177, 1975.

[41] K. Fukushima, "Neocognitron: A self-organizing neural network model for a mechanism of pattern recognition unaffected by shift in position," *Biological cybernetics*, vol. 36, no. 4, pp. 193–202, 1980.

[42] Y. LeCun, B. Boser, J. S. Denker, D. Henderson, R. E. Howard, W. Hubbard, and L. D. Jackel, "Backpropagation applied to handwritten zip code recognition," *Neural computation*, vol. 1, no. 4, pp. 541–551, 1989.

[43] S. Hochreiter and J. Schmidhuber, "Lstm can solve hard long time lag problems," in *Advances in neural information processing systems*, 1997, pp. 473–479.

[44] H. Sak, A. Senior, and F. Beaufays, "Long short-term memory recurrent neural network architectures for large scale acoustic modeling," in *Fifteenth annual conference of the international speech communication association*, 2014.

[45] G. E. Hinton and R. R. Salakhutdinov, "Reducing the dimensionality of data with neural networks," *science*, vol. 313, no. 5786, pp. 504–507, 2006.

[46] S. Lohr, "The age of big data," *New York Times*, vol. 11, no. 2012, 2012.

[47] V. Mnih, K. Kavukcuoglu, D. Silver, A. Graves, I. Antonoglou, D. Wierstra, and M. Riedmiller, "Playing atari with deep reinforcement learning," *arXiv preprint arXiv:1312.5602*, 2013.

[48] Y. Bengio, A. Courville, and P. Vincent, "Representation learning: A review and new perspectives," *IEEE transactions on pattern analysis and machine intelligence*, vol. 35, no. 8, pp. 1798–1828, 2013.

[49] A. Krizhevsky, I. Sutskever, and G. E. Hinton, "Imagenet classification with deep convolutional neural networks," in *Advances in neural information processing systems*, 2012, pp. 1097–1105.

[50] C. Farabet, C. Couprie, L. Najman, and Y. LeCun, "Learning hierarchical features for scene labeling," *IEEE transactions on pattern analysis and machine intelligence*, vol. 35, no. 8, pp. 1915–1929, 2013.

[51] K. Simonyan and A. Zisserman, "Very deep convolutional networks for large-scale image recognition," *arXiv preprint arXiv:1409.1556*, 2014.

[52] C. Szegedy, W. Liu, Y. Jia, P. Sermanet, S. Reed, D. Anguelov, D. Erhan, V. Vanhoucke, and A. Rabinovich, "Going deeper with convolutions," in *Proceedings of the IEEE conference on computer vision and pattern recognition*, 2015, pp. 1–9.

[53] K. He, X. Zhang, S. Ren, and J. Sun, "Deep residual learning for image recognition," in *Proceedings of the IEEE conference on computer vision and pattern recognition*, 2016, pp. 770–778.

[54] S. Zagoruyko and N. Komodakis, "Wide residual networks," *arXiv preprint arXiv:1605.07146*, 2016.

[55] S. Xie, R. Girshick, P. Dollár, Z. Tu, and K. He, "Aggregated residual transformations for deep neural networks," in *Proceedings of the IEEE Conference on Computer Vision and Pattern Recognition*, 2017, pp. 1492–1500.

[56] Y. LeCun, K. Kavukcuoglu, C. Farabet, *et al.*, "Convolutional networks and applications in vision.," in *ISCAS*, vol. 2010, 2010, pp. 253–256.

[57] N. Hatipoglu and G. Bilgin, "Cell segmentation in histopathological images with deep learning algorithms by utilizing spatial relationships," *Medical & Biological Engineering & Computing*, vol. 55, no. 10, pp. 1829–1848, 2017.

[58] S. L. Phung and A. Bouzerdoum, "Matlab library for convolutional neural networks," *University of Wollongong, Tech. Rep., URL: http://www. elec. uow. edu. au/staff/sphung*, 2009.

[59] J. Salamon and J. P. Bello, "Deep convolutional neural networks and data augmentation for environmental sound classification," *IEEE Signal Processing Letters*, vol. 24, no. 3, pp. 279–283, 2017.

[60] A. Cossarizza, H.-D. Chang, A. Radbruch, M. Akdis, I. Andrä, F. Annunziato, P. Bacher, V. Barnaba, L. Battistini, W. M. Bauer, *et al.*, "Guidelines for the use of flow cytometry and cell sorting in immunological studies," *European journal of immunology*, vol. 47, no. 10, pp. 1584–1797, 2017.

[61] P. Kamavisdar, S. Saluja, and S. Agrawal, "A survey on image classification approaches and techniques," *International Journal of Advanced Research in Computer and Communication Engineering*, vol. 2, no. 1, pp. 1005–1009, 2013.

[62] H. Su, "Nuclei cell detection in microscopic skeletal muscle fiber images and histopathological brain tumor images using sparse optimizations," 2014.

[63] Y. Chen, H. Jiang, C. Li, X. Jia, and P. Ghamisi, "Deep feature extraction and classification of hyperspectral images based on convolutional neural networks," *IEEE Transactions on Geoscience and Remote Sensing*, vol. 54, no. 10, pp. 6232–6251, 2016.

[64] K. Mizuno, Y. Terachi, K. Takagi, S. Izumi, H. Kawaguchi, and M. Yoshimoto, "Architectural study of hog feature extraction processor for real-time object detection," in *2012 IEEE Workshop on Signal Processing Systems*, IEEE, 2012, pp. 197–202.

[65] A. Cruz-Roa, J. C. Caicedo, and F. A. González, "Visual pattern mining in histology image collections using bag of features," *Artificial intelligence in medicine*, vol. 52, no. 2, pp. 91–106, 2011.

[66] X. Wen, L. Shao, W. Fang, and Y. Xue, "Efficient feature selection and classification for vehicle detection," *IEEE Transactions on Circuits and Systems for Video Technology*, vol. 25, no. 3, pp. 508–517, 2015.

[67] Y. Guo, Y. Liu, A. Oerlemans, S. Lao, S. Wu, and M. S. Lew, "Deep learning for visual understanding: A review," *Neurocomputing*, vol. 187, pp. 27–48, 2016.

[68] L. K. Hansen and P. Salamon, "Neural network ensembles," *IEEE Transactions on Pattern Analysis & Machine Intelligence*, no. 10, pp. 993–1001, 1990.

[69] T. S. Furey, N. Cristianini, N. Duffy, D. W. Bednarski, M. Schummer, and D. Haussler, "Support vector machine classification and validation of cancer tissue samples using microarray expression data," *Bioinformatics*, vol. 16, no. 10, pp. 906–914, 2000.

[70] A. Khammari, F. Nashashibi, Y. Abramson, and C. Laurgeau, "Vehicle detection combining gradient analysis and adaboost classification," in *Proceedings. 2005 IEEE Intelligent Transportation Systems, 2005.*, IEEE, 2005, pp. 66–71.

[71] B. Pepik, M. Stark, P. Gehler, and B. Schiele, "Teaching 3d geometry to deformable part models," in *2012 IEEE conference on computer vision and pattern recognition*, IEEE, 2012, pp. 3362–3369.

[72] N. Aloysius and M. Geetha, "A review on deep convolutional neural networks," in *2017 International Conference on Communication and Signal Processing (ICCSP)*, IEEE, 2017, pp. 0588–0592.

[73] E. D. Gelasca, B. Obara, D. Fedorov, K. Kvilekval, and B. Manjunath, "A biosegmentation benchmark for evaluation of bioimage analysis methods," *BMC Bioinformatics*, vol. 10, no. 1, p. 368, 2009.

[74] R. Suganya and R. Shanthi, "Fuzzy c-means algorithm-a review," *Int. Journal of Scientific and Research Publications*, vol. 2, no. 11, p. 1, 2012.

[75] J. C. Dunn, "A fuzzy relative of the isodata process and its use in detecting compact well-separated clusters," 1973.

[76] J. C. Bezdek, *Pattern recognition with fuzzy objective function algorithms*. Springer Science & Business Media, 2013.

[77] Y. Xie, F. Xing, X. Kong, H. Su, and L. Yang, "Beyond classification: Structured regression for robust cell detection using convolutional neural network," in *International Conference on Medical Image Computing and Computer-Assisted Intervention*, Springer, 2015, pp. 358–365.

[78] M. Kuse, Y.-F. Wang, V. Kalasannavar, M. Khan, and N. Rajpoot, "Local isotropic phase symmetry measure for detection of beta cells and lymphocytes," *Journal of pathology informatics*, vol. 2, 2011.

[79] Y. Yuan, H. Failmezger, O. M. Rueda, H. R. Ali, S. Gräf, S.-F. Chin, R. F. Schwarz, C. Curtis, M. J. Dunning, H. Bardwell, *et al.*, "Quantitative image analysis of cellular heterogeneity in breast tumors complements genomic profiling," *Science translational medicine*, vol. 4, no. 157, 157ra143–157ra143, 2012.

[80] V. A. Sindagi and V. M. Patel, "Generating high-quality crowd density maps using contextual pyramid cnns," in *Proceedings of the IEEE International Conference on Computer Vision*, 2017, pp. 1861–1870.

[81] W. Shao, L. Sun, and D. Zhang, "Deep active learning for nucleus classification in pathology images," in *IEEE 15th International Symposium on Biomedical Imaging, ISBI'18*, IEEE, 2018, pp. 199–202.

[82] K. Mohan, P. Chandrasekhar, and S. Jilani, "Fuz-SVM classifier based object face liveness detection with combined hog-lpq," *Int. Journal of Engineering Research and Development*, vol. 12, no. 12, pp. 01–09, 2016.

[83] V. Ojansivu and J. Heikkilä, "Blur insensitive texture classification using local phase quantization," in *International conference on image and signal processing*, Springer, 2008, pp. 236–243.

[84] C. Cortes and V. Vapnik, "Support-vector networks," *Machine Learning*, vol. 20, no. 3, pp. 273–297, 1995.

[85] A. F. Agarap, "An architecture combining convolutional neural network (CNN) and support vector machine (SVM) for image classification," *arXiv preprint arXiv:1712.03541*, 2017.

[86] F. A. Spanhol, L. S. Oliveira, C. Petitjean, and L. Heutte, *Breast cancer histopathological image classification using convolutional neural networks*, IEEE, 2016.

Publications From the Thesis

Contact Information: f0115069@std.yildiz.edu.tr

Conference Papers

1. Alah, R.; Bilgin, G. and Albayrak, A. (2019). Automatic Nuclei Detection in Histopathological Images based on Convolutional Neural Networks.In Proceedings of the 12th International Joint Conference on Biomedical Engineering Systems and Technologies - Volume 4: BIOSIGNALS, ISBN 978-989-758-353-7, pages 193-200. DOI: 10.5220/0007484301930200

2. Abed Alah R.S., Bilgin G., "Nuclei Classification in Histopathological Images via Local Phase Quantization and Convolutional Neural Networks", Elektrik-Elektronik, Bilgisayar, Biyomedikal Mühendislikleri Bilimsel Toplantısı EBBT'19, Scientific Meeting on Electrical-Electronics, Computer Science, Biomedical Engineering, İSTANBUL, TÜRKIYE, 24-26 Nisan 2019, pp.1-4